

---

# Sédimentation Grand Bassam

## Exploration de mesures de mitigation

-

# Rapport

-

---

Authors:	Dano Roelvink	Unesco-IHE
	Cilia Swinkels	Deltares
	Robert Hasselaar	Deltares
	Marten Hillen	RoyalHaskoningDHV



# 1 Introduction

## 1.1 Problem statement

At the city of Grand-Bassam (Côte d'Ivoire) there is currently no sustainable connection between the Ébrié lagoon and the Atlantic Ocean. This results in an increased risk of flooding during high river discharges and has had a negative impact on the water quality in the region. Potential economic development in the tourism and fishery sector cannot develop due to lack of this connection with the ocean.

Several attempts to open this access channel were conducted in the last decades (see Figure 1). The channel connecting Grand-Bassam (Côte d'Ivoire) with the Atlantic Ocean silted on all of these occasions. Longshore sediment transport is seen as the main reason for this sedimentation. In this note engineering measures are explored and presented to connect the channel at Grand-Bassam with the Atlantic Ocean.



Royal HaskoningDHV was asked to draft conceptual designs for connecting the lagoon with the ocean. Other potential measures to address the challenges at Grand-Bassam were not evaluated and are outside the scope of this memo.

Figure 1: Aerial photo channel Grand-Bassam (1989)

## 1.2 Approach

The research institute Deltares developed a set of numerical models to evaluate the hydrodynamics of the Ébrié lagoon and the coastal and lagoon dynamics around Grand-Bassam. The model outcomes and further insight in the systems dynamics from literature served as input for Haskoning to define a number of conceptual engineering measures to open the access channel at Grand Bassam. The measures were evaluated in an engineering expert meeting regarding three criteria:

1. effectiveness in local conditions
2. technical complexity for implementation
3. expected construction, operation and maintenance costs.

Based on these criteria, four alternatives were selected, which were subsequently assessed with the Deltares morphodynamic model for a dry season scenario. From the model results, the morphological

development of the inlet for the different alternatives is computed and conclusions are drawn on the preferred alternative based on its effectiveness in maintaining Grand Bassam inlet open.

### **1.3 Structure du rapport**

Après l'Introduction, dans Chapitre 2 nous donnons une brève description du système de l'embouchure de Grand Bassam connectant le système lagunaire et fluvial avec l'Océan.

En Chapitre 3 nous présentons les mesures conceptuelles avec leurs avantages et inconvénients et leurs aspects pratiques.

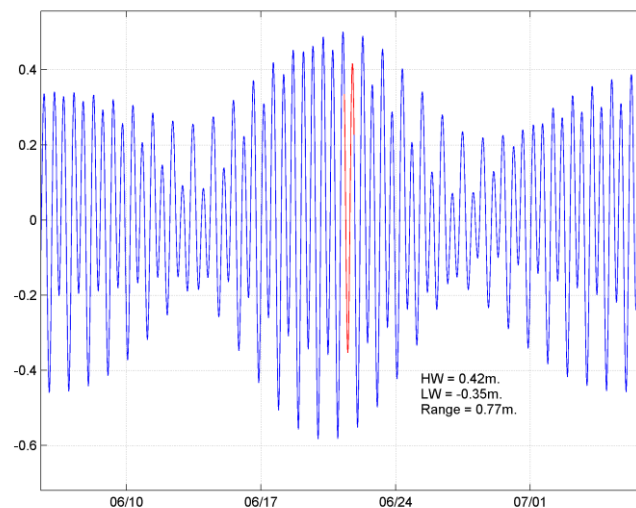
Chapter 4 presents the model evaluation of the proposed alternatives.

## 2 Description du système

### 2.1 Marée

La marée est caractérisée par un régime micro-tidale. Elle est semi-diurne avec une inégalité diurne. Le marnage est entre 1.1 m à vive eau et 0.4 m à morte eau.

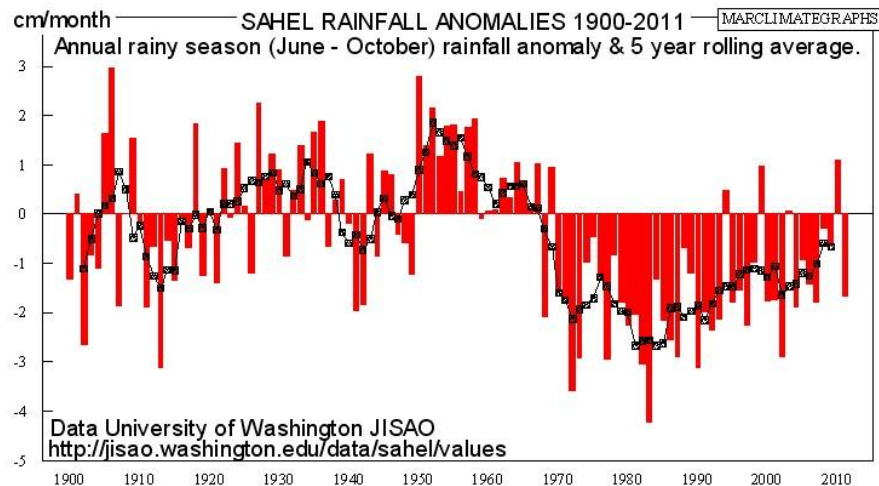
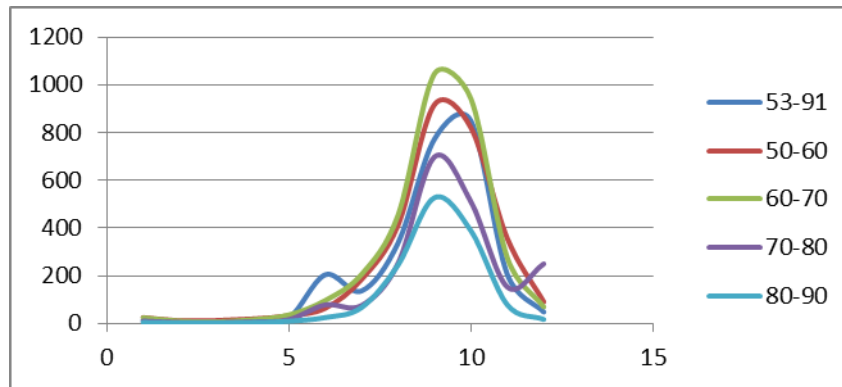
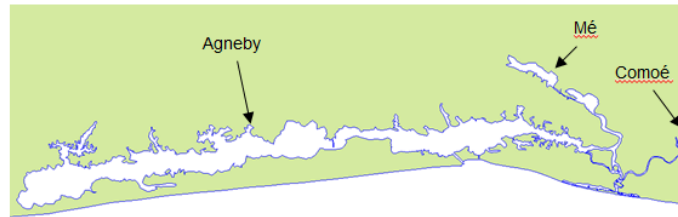
Dans la vaste et peu profonde Lagune d'Ebrié la marée est réduite beaucoup et ne surpasse pas quelques décimètres près de Grand Bassam.



### 2.2 River discharges

Three main rivers discharge into the Ebrié estuary: the Mé, Agneby and Comoé. The Agneby and the Mé are rivers with an equatorial runoff regime. The wet season falls in the months June to August, when the average discharge of both rivers is approximately 50 m<sup>3</sup>/s. The average discharge in the dry season is 12.5 m<sup>3</sup>/s. The Comoé is a river with a tropical regime that drains part of the southern Sahel region. The wet season falls in the months September to November with an average wet season discharge of 550 m<sup>3</sup>/s. Historically, wet season run off rates were much higher, with average peak discharges upto 1100 m<sup>3</sup>/s. A significant decrease in wet season runoff was observed over the last decades, which is presumably related to a drier period in the Sahel since the 1970's. It is not quite clear whether this is a

continuous trend or caused by a decadal climate oscillation; climate projections for the region show no consensus on this matter.

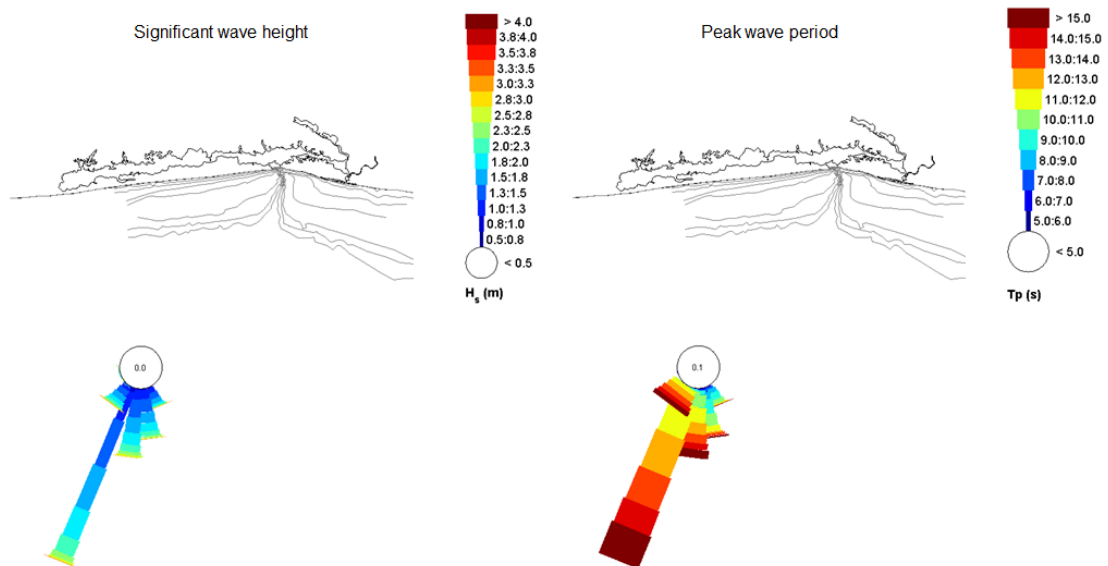


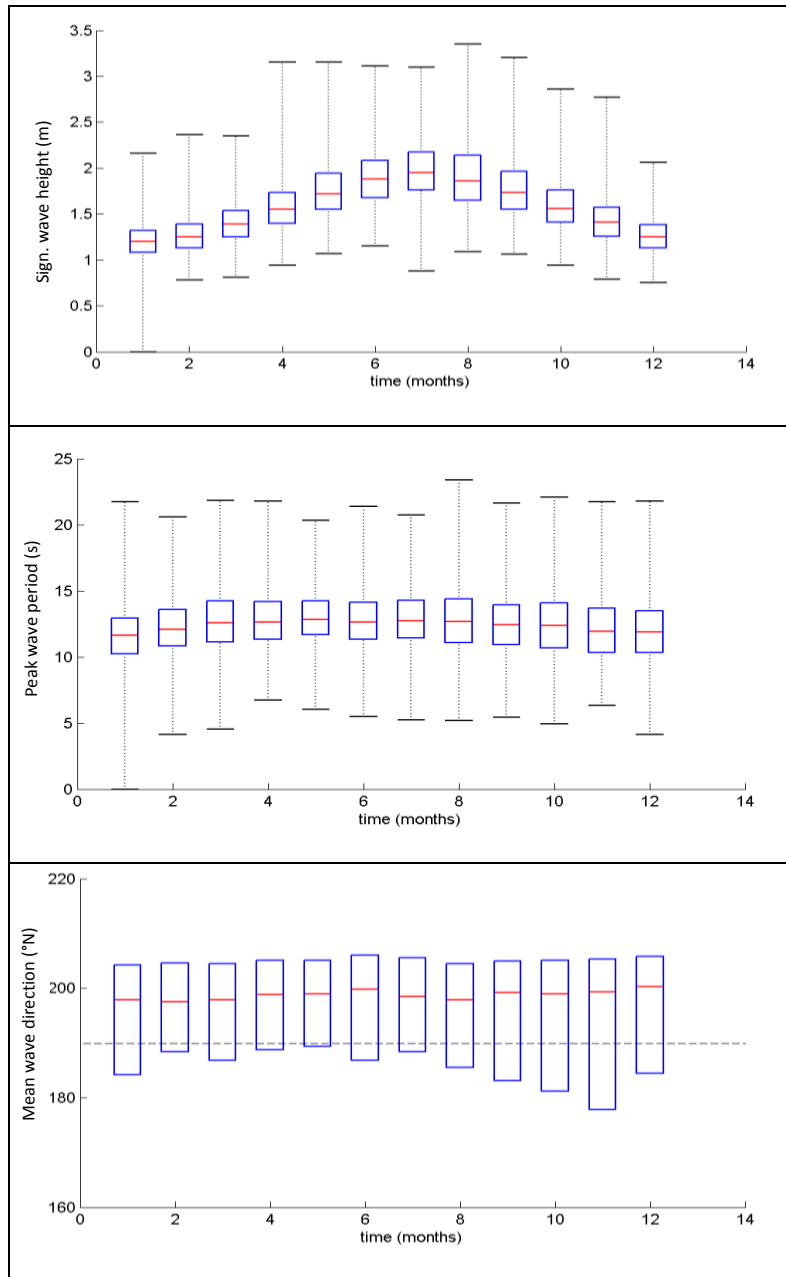
## 2.3 Wave climate

The wave climate off the Ivorian coast is characterized by long swells coming from the south to southwest sector. These swells originate in the Southern Atlantic Ocean and travel 1000's of kilometres before hitting the coast of Northern Africa. Locally, sea breezes generate smaller, shorter period wind waves that are superimposed on the swell wave climate.

Most waves arrive from the south to southwest sector, with average wave directions typically between 160 and 220°N. The highest waves occur between May and August, with a mean significant wave height upto 2m and mean peak wave period between 10 and 14 s. In the months September to November, the wave climate is characterized by slightly lower wave heights and more southerly wave directions.

The wave roses presented in Figure xx are based on 30 year of hindcast data (1979 to 2009) from the NOAA WaveWatch III model. The roses clearly illustrate the long period dominated wave climate and the narrow directional sector from which wave energy approaches the Ivorian coastline.





## 2.4 Sediment characteristics and littoral transport

According to Laurent *et al* (1996), in the Comoe river mouth, the grain size increases from the high intertidal zone (525  $\mu\text{m}$  on average) to the low intertidal zone (918  $\mu\text{m}$  on average), see table below.

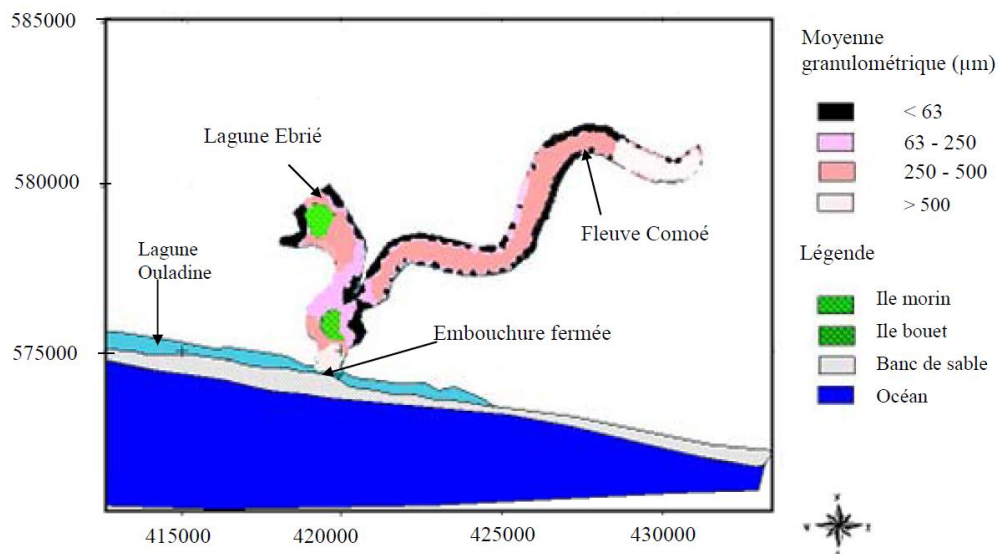


Tableau 1. Granulometry of sands in Comoé river mouth.

	Mean granulometric dimensions ( $\mu\text{m}$ )				
	Minimum	Maximum	Average	Standard deviation	
Estuary	67	765	329	231.12	
Beach	High intertidal zone	469	708	525	86.34
	Mid intertidal zone	532	824	756	74.57
	Low intertidal zone	863	1012	918	62.60

The bed material in the lagoon consists of muddy fine sediments with high content of organic matter. Along the estuary banks, muddy deposits are presents while in the middle of the branches, sand/mud mixture and fine sands are present (see Figure below).

Figure 2: Répartition des faciès de surface des sédiments dans l'estuaire du fleuve Comoé



According to literature, the beach material along the Grand Bassam coastline consists of medium to coarse sands. The reported D50 shows large variations; from 300 to 900  $\mu\text{m}$ . The beach profile near Grand Bassam was measured in the year 1986 (Abe, 2005) and has an average nearshore slope of approximately 1:10.

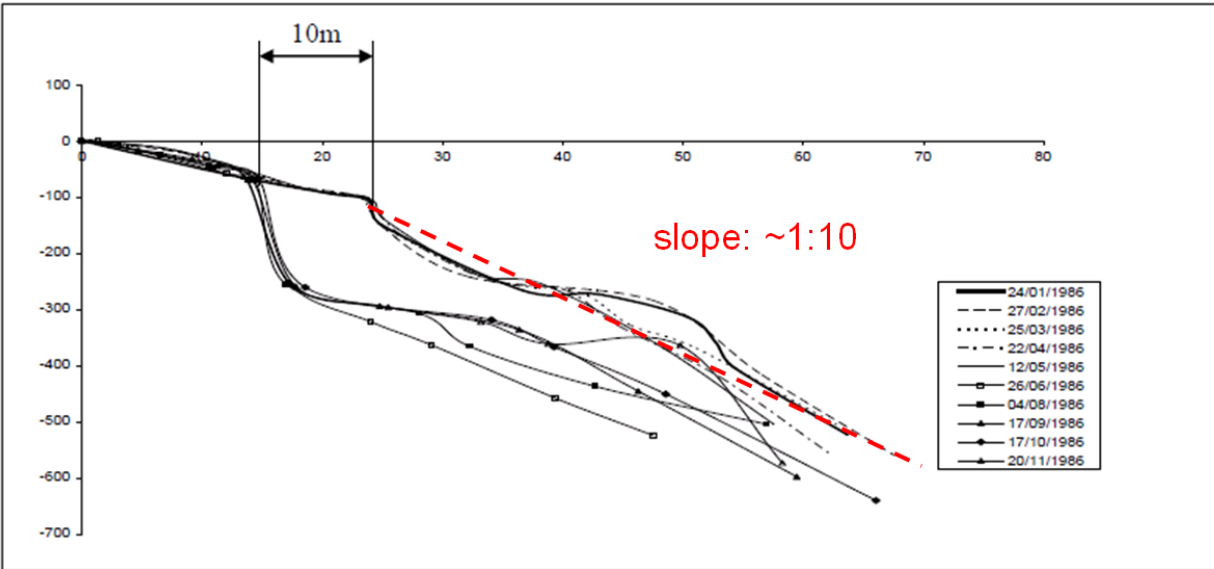


Figure 57 : Profil de plage au PK23, route de Bassam, 1986

From a literature review, limited information or field data on sediment transport rates and transport directions along the Ivorian coastline is found. However, it is known that the long period waves coming from the S-SW directional sector lead to strong littoral transports. Sogreah (2000) estimated the littoral transport west of Abidjan harbour between 700.000 – 1.100.000 m<sup>3</sup>/yr, based on the observed sedimentation against the harbour breakwaters of Canal Vridi. Due to the S-SW wave incidence, the littoral transport along this stretch of coastline is considered to be practically unidirectional directed to the East.

Because of the lower angle of incidence, Sogreah estimates the littoral transport at Grand Bassam at 400.000 – 650.000 m<sup>3</sup>/yr in eastward direction. This estimate is solely based on a translation from the transport rates observed West of Vridi to Grand Bassam and is not supported by field observations. Therefore, the presented number should be treated with care.

Historical aerial photographs of the Grand Bassam inlet show the formation of spit-like features (*fleches*) in the inlet, that are present both on the eastern and western shore (see figure below). This suggests that the sediment transport direction along the Grand Bassam coastline is bi-directional.

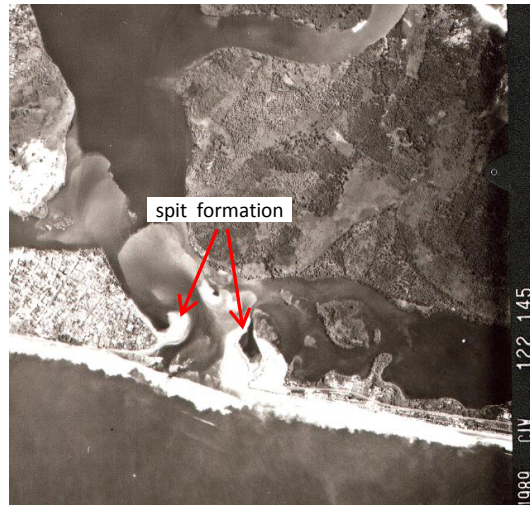


Photo aérienne 1989 – courtoisie BNETD/CCT



## 2.5 Grand Bassam Inlet

In the past, several attempts have been done to re-open the Grand Bassam inlet. However, le débit en saison sèche de la Comoé est de 5 m<sup>3</sup>/s contre 550 m<sup>3</sup>/s en saison des pluies et en saison sèche le flot devient insuffisant pour ouvrir l'embouchure. La fermeture de l'embouchure est inéluctable sans aménagement.

The below table presents a brief overview of the historic (artificial) openings of the Grand Bassam Inlet and associated estimates of dredged volumes.

Historique des ouvertures et observations (Lombardo, 2010):

- **1987** : chenal 820 x 40 x 4. Dragage de **105 000 m<sup>3</sup>** à **130 M CFA**.

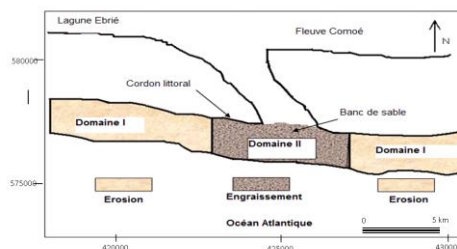
Ouverte de Sept 87 à Août 89 (23 mois). Largeur passée à 150 m le 5.10.87

- **1992** : Chenal de 890 m, dragage de **250 000 m<sup>3</sup>** à **220 M. CFA** . (7 mois d'ouverture)
- **1997** : Percement d'un nouveau chenal, colmaté la même année
- **1998** : Nouveau chenal entretenu jusqu'en 1999 par le Port d'Abidjan
- **2001** : demi chenal avec bouchon de 60 m formant un verrou de 1,5 m de large
- **2009** : forte sédimentation par l'Océan (de plus de 3 m) en 5 mois dans le chenal sur toute sa longueur, représentant 80 000 m<sup>3</sup> de dépôts

Considering the above information combined with the analysis presented in the table below (source xx), the sedimentation at Grand Bassam is estimated at 200.000 – 400.000 m<sup>3</sup> per year, caused by sediment transport from both the eastern and the western side.

Périodes	Juin - Juil	Août - Sept	Oct - Nov	Mar - Avr.	Total des volumes
Surface érodée (m <sup>2</sup> )	59,28	60,91	102,93	77,19	300,31
Surface engraisée (m <sup>2</sup> )	75,16	231,9	63,88	187,9	558,84
Volume de sable déplacé (m <sup>3</sup> )	11856	12182	20586	15438	<b>-60062</b>
Volume de sable déposé (m <sup>3</sup> )	74812	168680	12776	165260	<b>+421528</b>
Différence (m <sup>3</sup> )	+62956	+156498	-7810	+149822	<b>+361466</b>
Tendance évolutive	Dépôt	Dépôt	Erosion	Dépôt	

**Tableau:** accumulées Estimation du volume total de sables (Juin 2006 à Avril 2007 des 7 stations)



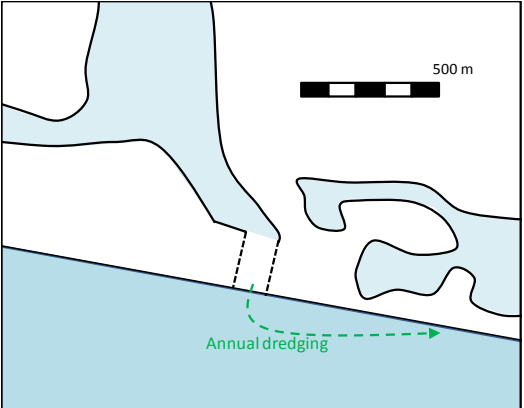

### 3 Mesures conceptuelles

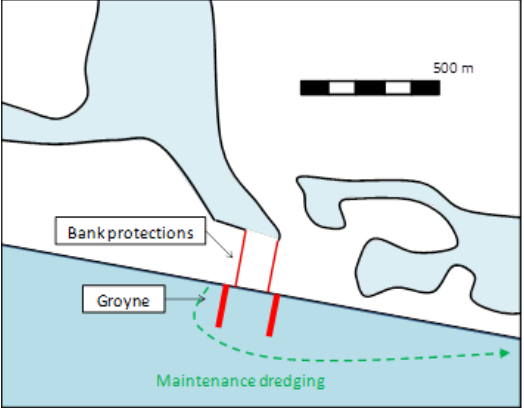


This reconnaissance study evaluates several concepts based on previous model studies, limited data on the hydraulic boundary conditions and historic attempts to connect the Ébrié lagoon and the Atlantic Ocean via a(n) (access) channel. In drafting these conceptual designs the following basic assumptions are made:

- The longshore sediment transport is mainly caused by swell from the Atlantic Ocean;
- The net sediment transport direction is in Eastern direction;
- Due to the dynamic environment at Grand-Bassam, both Westward and Eastward sediment transport are significant;
- Tide (and the basin size) and river flow are considered too small to keep the access channel open in the current situation;
- The bridge land inward from the opening does not allow for (large) dredging equipment; therefore this equipment can only enter Grand Bassam from the ocean side.

Before evaluating the outcomes of modelling the different alternatives, the following *a priori* assessment can be made:

	<p><u>0. Create an opening before every rain season</u>          Flooding due to high river flows can be solved fairly straightforward. A small channel can be dug before a flood arrives and the water will widen the small channel itself. This work could be done by a few bulldozers. Water quality will then improve for a short period until the opening is filled again with sand due to longshore sediment transport. This work could be done with local equipment.</p> <p>Pros:</p> <ul style="list-style-type: none"> <li>• Minimal costs</li> <li>• Low impact on coastal profile</li> <li>• Work can be done with local equipment</li> <li>• Local straightforward implementation.</li> </ul> <p>Cons:</p>
--	--

	<ul style="list-style-type: none"> <li>• Not effective all year, does not answer the water quality challenge (additional measures may be required)</li> <li>• Opening only for a short period during the year</li> </ul>
 	<p><u>1. Annual dredging (only)</u></p> <p>In this solution the channel is dredged annually. No additional engineering measures are constructed. Based on the sedimentation numbers from the Sogreah reports (2000), it is estimated that 200,000 to 400,000 m<sup>3</sup> will have to be dredged annually. As the net longshore sediment transport (from West to East), the dredged material should be deposited along the coast East from the channel. In this way additional erosion of the coastline is prevented. Initial re-opening of the channel should probably be executed by a larger dredging vessel such as a (small) cutter suction dredger. This work will take a few weeks to a few months, depending on the size and type of equipment. Maintenance dredging could be performed with a hopper dredger, if there is sufficient channel depth; otherwise, a backhoe or cutter dredger is necessary.</p> <p>Pros:</p> <ul style="list-style-type: none"> <li>• low investments costs</li> <li>• leese side erosion problems limited</li> <li>• Straightforward construction method</li> <li>• Maintenance dredging expected to be most suitable for capacity building of contractors in Cote d'Ivoire</li> <li>• As this is a 'soft' engineering measure, it allows for an adaptive sedimentation policy</li> </ul> <p>Cons:</p> <ul style="list-style-type: none"> <li>• channel stability very low, channel likely to migrate</li> <li>• high maintenance dredging costs</li> <li>• required dredging frequency for maintaining the channel. The amount of dredging will strongly depend on yearly wave and current</li> </ul>

	<p>conditions</p> <ul style="list-style-type: none"> <li>• Keeping the required depth of the channel appropriate for shipping will require intensive maintenance.</li> </ul>
  	<p><u>2. Groynes</u></p> <p>With this solution groynes combined with bank protections are proposed to block the longshore sediment transport. The groynes will have to be protected with large blocks (for instance acropods) to resist wave attack (comparable to Canal de Vridi; see figure 2). Engineering has to be optimized during feasibility study and detailed design phase.</p> <p>To stabilize the channel's location (parallel to the coast), bank protections are constructed. Due to the construction of the groynes, sediment will accumulate west of the groynes. East from the channel the coast will erode. Sand by-passing will be required to prevent erosion of the coast east of the channel. Furthermore, maintenance dredging in the channel is required as physical model studies (Sogreah, 2000) show significant sedimentation in the channel.</p> <p>The Eastern groyne is required to prevent westward sediment transport. Whether or not this groyne is required is yet unknown at this stage. Hydrodynamic modelling could clarify this.</p> <p>Initial re-opening of the channel can be executed with a small cutter dredger or a backhoe. The groyne and bank protections can be constructed with land based equipment. A cutter dredger or backhoe is required for by-passing of sand. Dredging of the access channel will take weeks to a couple of months depending on weather conditions. Construction of the groynes requires detailed design to be conducted during a feasibility study and construction can take up to 6 months, depending on wave conditions (and</p>



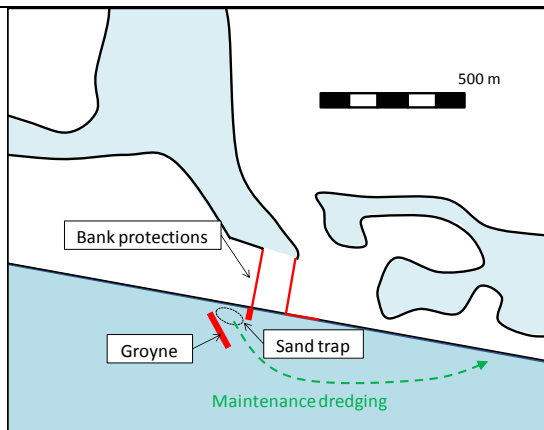
down time of equipment).

Pros:

- less frequent dredging and therefore lower maintenance costs
- channel width/depth can be optimized for shipping and in and outflow of the backwaters;

Cons:

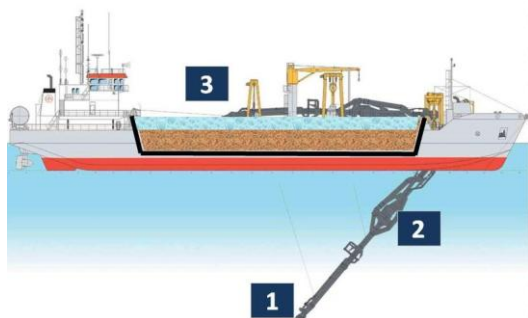
- high investment costs
- leeside erosion (sand by-passing necessary)
- cutter dredger or backhoe needed for by-passing of sand.



### 3. Off-shore groyne with sand trap

With this solution an off-shore groyne is constructed west of the channel to reduce the wave-induced sediment transport. Groyne design likely requires large acropods and or block protection to prevent erosion due to wave attack (Hs: 1.5m, Tp: 12.5s). Sedimentation in a (man-made) sand trap (pit) will occur and prevent sedimentation of the channel. The sand trap can be emptied with a hopper dredger. Sand by-passing will be required to prevent erosion of the coast east of the channel.

Again bank protections are constructed to prevent movement of the channel (parallel to the coast).



Initial re-opening of the channel can be executed with a small cutter dredger or a backhoe. The groyne has to be constructed with waterborne equipment. The bank protections can be made with landbased equipment. A hopper dredger can by-pass sand. This work will take a few months to a year, depending on the type of equipment and the time available for construction (down time). Due to the use of waterborne equipment the downtime of this option will be larger than option 2 (groynes).



	<p>Pros:</p> <ul style="list-style-type: none"> <li>• channel width/depth can be optimized for shipping and in and outflow of the backwaters;</li> <li>• less frequent dredging and therefore lower maintenance costs</li> <li>• sand trap can be emptied by hopper dredger (similar equipment as is applied for dredging the port of Abidjan) and by-passed.</li> <li>• limited influence on coastline</li> </ul> <p>Cons:</p> <ul style="list-style-type: none"> <li>• Feasibility of this option is uncertain due to the highly dynamic sediment transport conditions and because Westward sediment transport is not blocked in this conceptual design.</li> <li>• high(er) investment costs;</li> <li>• leeside erosion (sand by-passing necessary)</li> </ul>
--	--

Among the options which were also considered were;

- Permanent dredging installation: an installation which permanently dredges material from the proposed channel location. Unpredictable sediment dynamics require high-end engineering to set up this proposed measures. Furthermore, operating and maintaining this type of installation is costly and will require well trained staff.
- Pipe line: A pipe line can connect water of the Atlantic Ocean with that of Grand-Bassam. It could solve the water quality issue, but does not allow for shipping and does not solve flooding. This option only partly solves the problem and for large quantities of water it will be a costly solution.

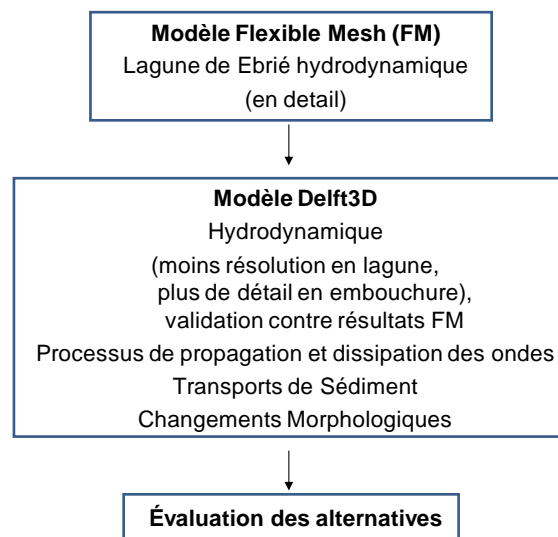
## 4 Mise en place des modèles et résultats

### 4.1 Approche

A set of hydrodynamic models is developed for the present study, which are used to assess the different alternatives for Grand Bassam. In a first step, a D-Flow Flexible Mesh (FM) model is set up to study the detailed hydrodynamics of the lagoon system. The recently developed D-Flow FM software allows for very flexible 2D gridding, making it possible to construct a detailed mesh that captures the full characteristics of the lagoon system. This is especially suitable for the complex geometry of Lagune Ebrié with its several tidal branches, islands and double inlet configuration.

As D-Flow FM does not yet allow for the modelling of waves and morphology, in a second step, a Delft3D model is set up. The model grid in this case does not capture the full detail of the lagoon, but is set up in such a way that it reproduces the main characteristics of the system (tidal storage capacity and distribution of discharges between the two inlets). The hydrodynamic results of the Delft3D model are validated against the detailed results of the D-Flow FM model.

Subsequently, wave processes, sediment transport and morphological updating are included in the validated Delft3D model. This fully morphodynamic model is used to study the morphodynamic evolution of Grand Bassam Inlet in detail and ultimately to assess the proposed measures to maintain the inlet open. The modelling approach is schematically shown in the chart below.



## 4.2 Modèle FM

### Model grid

The detailed FM model is set up with two objectives:

1. To reproduce the tidal propagation through the lagoon system
2. To investigate the inlet hydrodynamics at Canal Vridi and Grand Bassam and reproduce the distribution of tidal discharges over the two inlets

To achieve this, a FM model grid is set up with highest resolution in the two inlet regions to model the local hydrodynamics with sufficient detail, and coarser resolution offshore and inside the lagoon branches to resolve the tidal storage capacity of the lagoon (see Figure 4-1).

### Model bathymetry

The model bathymetry is constructed from the following data sources (in order of usage):

1. Depth survey conducted by IHE (region Grand Bassam, survey date xx-xx-2012, see Figure 4-2)
2. Admiralty Chart 3103 – Port d’Abidjan (1:10 000)
3. Admiralty Chart 3101 – Outer approaches to Port d’Abidjan (1:100 000)
4. Admiralty Chart 3100 – Sassandra to Lagune Aby (1:350 000)
5. Bathymetry as presented in Sogreah (2000)
6. Nearshore zone: Dean profile up to -20m MSL

It should be noted that only the survey conducted by IHE consists of detailed and recent information; all other sources are either coarse in resolution or typically based on surveys that were carried out before 1990.

By lack of survey data, assumptions have to be made on the dimensions on the Grand Bassam inlet. In literature, an average width of the channel of about 150m and average depth of about 3.5m are reported for the historic natural situation. These dimensions are therefore adopted in the model.

### Boundary conditions

The offshore sea boundaries are forced with tidal constituents derived from the Topex-Poseidon 7.2 Global Inverse Tide model. Initially, no river discharges are incorporated in the model. In the ultimate scenarios to evaluate the different alternatives, the run off of the rivers Agneby, Mé and Comoé are included in the model as total discharge imposed on the upstream boundaries.

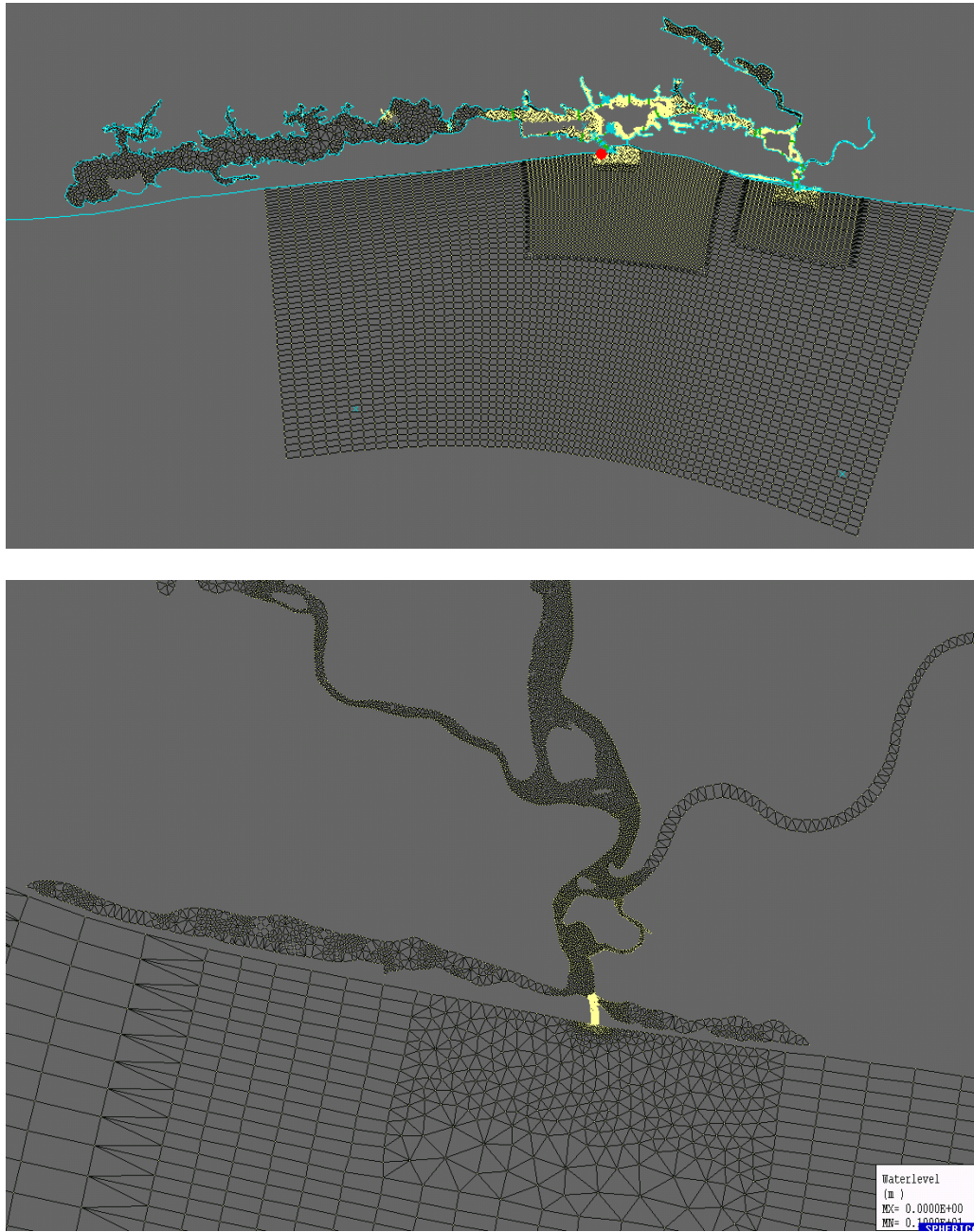


Figure 4-1 Full FM model grid domain (top) and detail at the Grand Bassam inlet with increased model resolution towards the inlet (bottom)

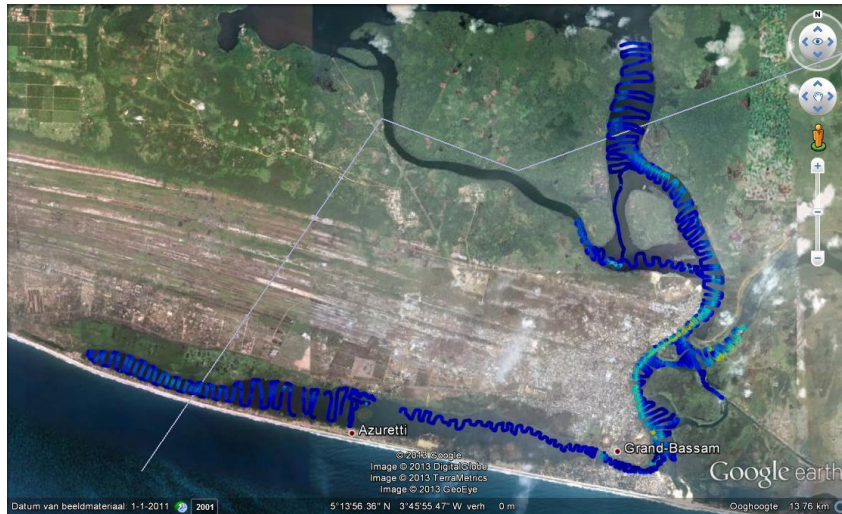


Figure 4-2 Measured bathymetry around Grand Bassam (IHE, 2012)

### Model validation

There is limited data available for validation of the model results levels. The only observed water level time series was found for the period 1982 to 1988 at Abidjan – Canal Vridi, downloaded from xxx. Furthermore, at the Port of Abidjan, the IHO constituents presented in Table 4-1 are known.

Figure 4-3 shows a comparison between the observed, predicted and modelled tidal water level at Canal Vridi. The three time series show good resemblance in main characteristics, such as the spring-neap cycle, diurnal inequality and tidal amplitude. In the model, no meteorological effects or river runoff was incorporated, which can explain (part of) the difference between the observed water levels and the model results. Qualitatively, the comparison shows that the tidal reproduction of the model from the offshore boundary to the entrance of the lagoon is adequate.

Constituent	Amplitude (m)	Phase (°)
K1	0.095	343.5
O1	0.014	321.4
P1	0.032	343.5
Q1	0.006	126.0
M2	0.286	139.9
S2	0.126	168.6
N2	0.073	134.5
K2	0.034	168.6

Table 4-1 IHO Observed tidal constants - Port of Abidjan

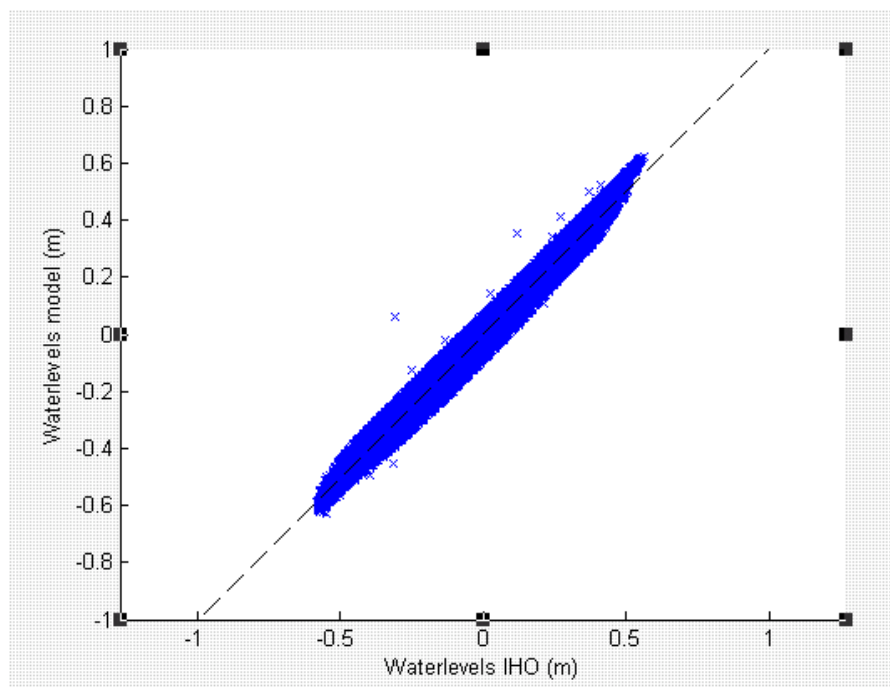
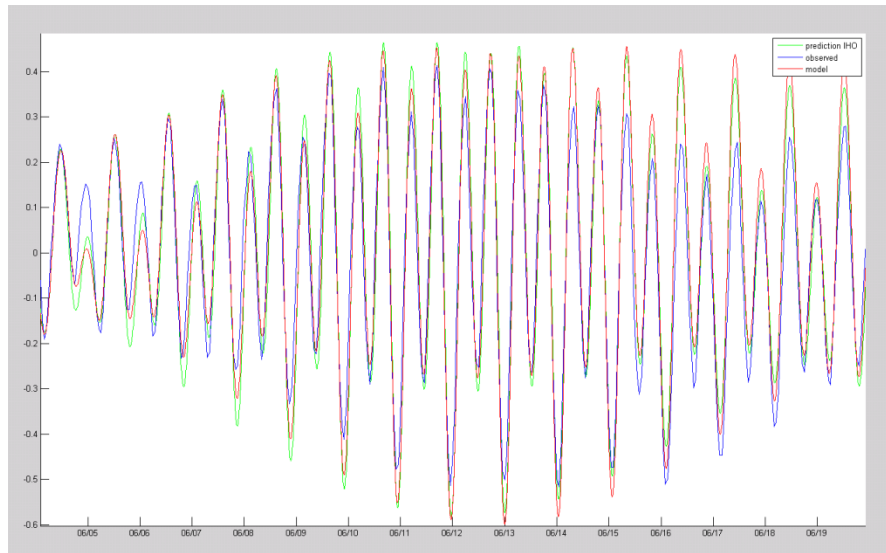


**Figure 4-3 Comparison of predicted, observed and modeled tidal water levels at Canal Vridi (top) and between predicted (IHO) and modeled water levels (bottom)**

To further validate the tidal propagation (tidal damping, phase shift) from the lagoon entrances towards the inland lagoon limits, information presented in Varlet (1978) is used. Varlet presents the tidal characteristics of the lagoon as the relation between the offshore tidal range near Canal Vridi and the tidal range at several locations inside the lagoon, as well as the phase shift in timing of High Water (HW) and Low Water (LW) between the offshore and inshore locations. This information is partly based on observations but largely empirically determined and should therefore be considered with caution. This information is presented in Figure 4-4.

From the Figure, it is found that the model matches the tidal damping of the system, as presented by Varlet, very well. Regarding phase shift of the high and low waters, there is a larger discrepancy between the model and the information presented by Varlet. However, Varlet mentions that the tidal retard is more difficult to determine than the tidal damping with the empirical method he uses, so this comparison has a lower significance.

Overall, it is concluded that the FM model represents the tidal propagation through Lagune Ebrié sufficiently accurate for the present exploratory modelling study. However, it is noted that the validation is based on limited data only and the model results therefore contain large uncertainty. If the model is to be used for more detailed studies in the near future, this aspect may have to be addressed again.

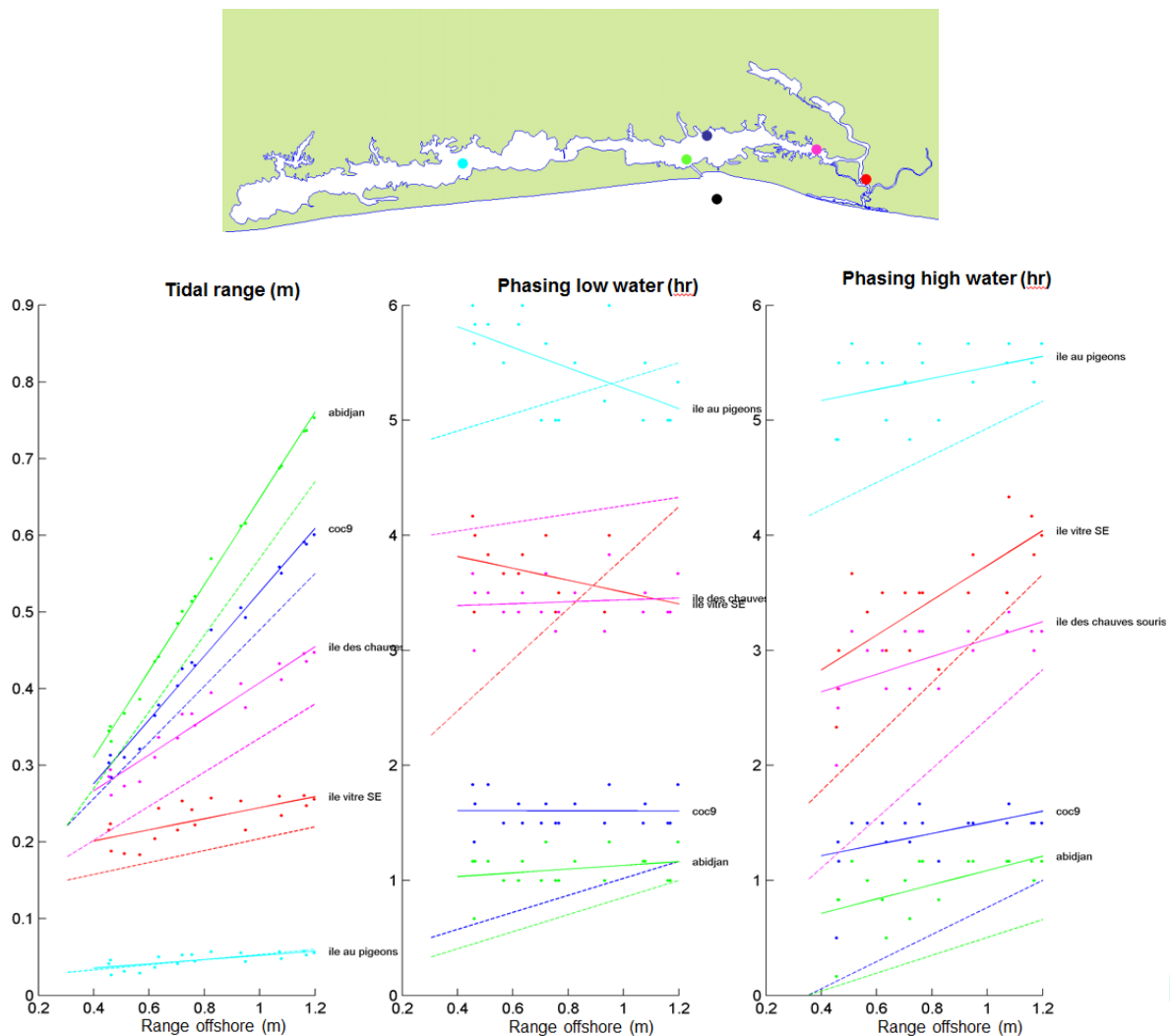


Figure 4-4 Comparison between ‘observed’ (dashed line, based on Varlet) and modeled (solid line) tidal water levels at several locations in Lagoon Ebrié, expressed as ratio between offshore tidal range and local tidal range (left), and in phase lag between offshore location and local station (mid and right). The colors of the lines match with the locations indicated in the top figure, whilst the offshore location is indicated by the black dot.



## Hydrodynamic results

Even though the tidal range dampens quickly away from the entrances of the lagoon, a large tidal volume passes the two inlets. The discharge through Grand Bassam inlet is found to be around 500-700 m<sup>3</sup>/s at spring tides (wet season, run off of Comoé is 550 m<sup>3</sup>/s). This is nearly 10% of the discharge passing Canal Vridi (~4000-5000 m<sup>3</sup>/s) because of the much smaller cross-sectional area of the Grand Bassam inlet (see Figure 4-5). By reducing the cross-sectional area of Grand Bassam inlet, which would naturally occur during siltation of the inlet, the discharge through Grand Bassam rapidly reduces to 0 m<sup>3</sup>/s. Very high flow velocities are observed in both inlets, with peak velocities during spring tides ranging up to 1.5 to 2 m/s (see Figure 4-6).

Figure 4-7 illustrates the flow velocities in Grand Bassam inlet over a spring-neap cycle, both for a wet season scenario (discharge Comoé = 550 m<sup>3</sup>/s) and a dry season scenario (discharge Comoé = 5 m<sup>3</sup>/s). The large difference between the ebb currents and flood currents in the wet season is clearly visible in this graph; it is this asymmetry that is considered to be responsible for scouring the inlet open during the wet season. The tidal asymmetry is less pronounced in the dry season, which can explain the sedimentation that mainly occurs during this period.

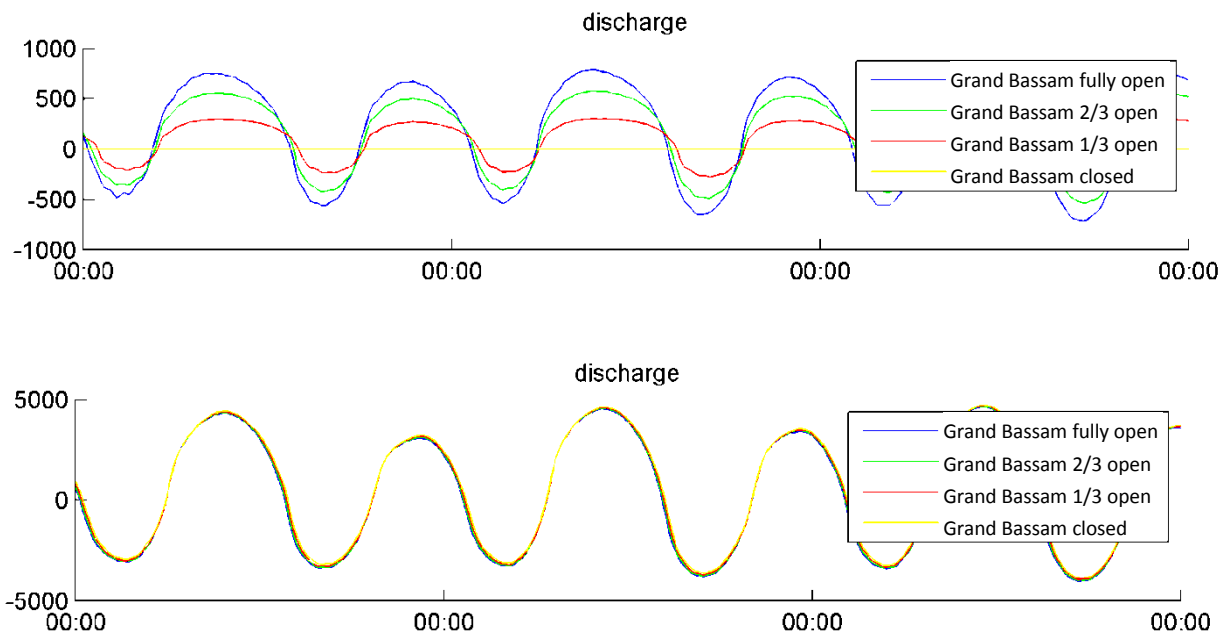


Figure 4-5 Instantaneous discharges through Canal Vridi (top) and Grand Bassam inlet (bottom) for different opening scenarios of Grand Bassam inlet.



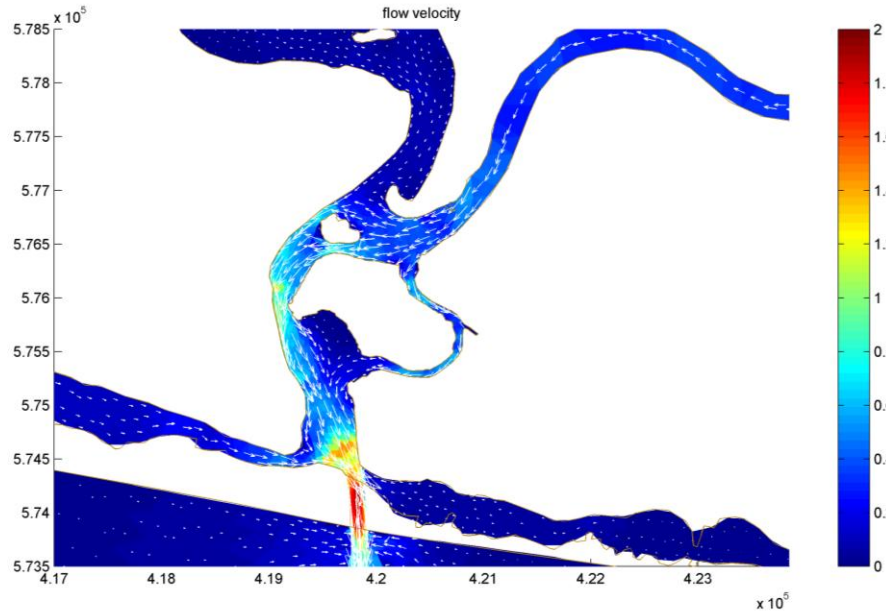


Figure 4-6 Flow velocities around Grand Bassam inlet at a moment of maximum ebb currents during a spring tide, wet season, Grand Bassam fully open.

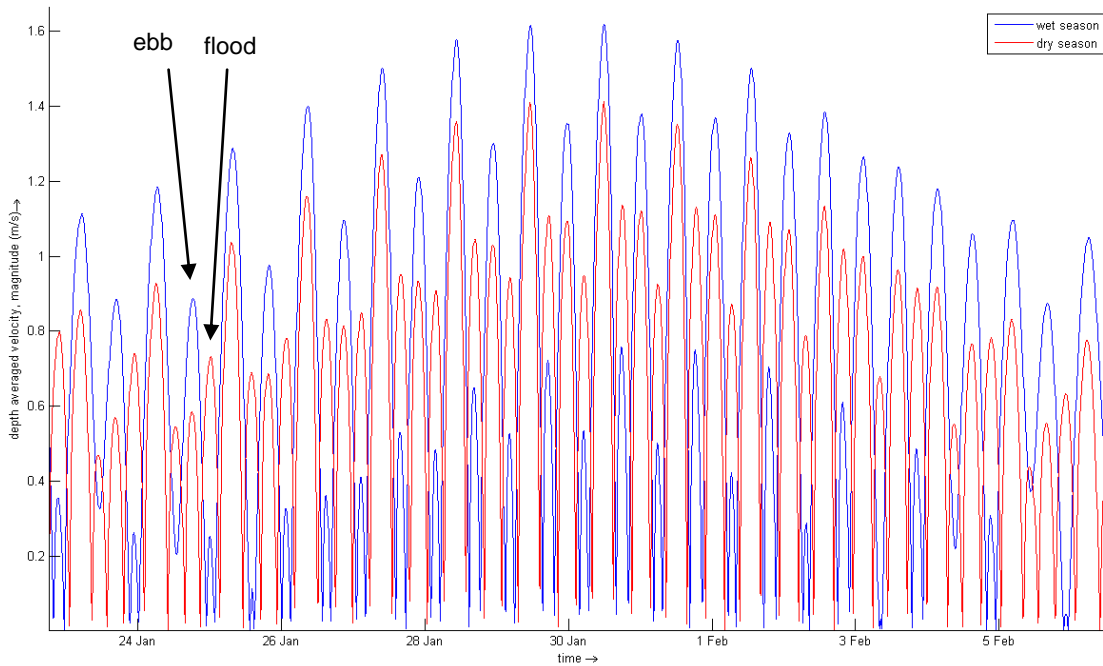


Figure 4-7 Modelled flow velocities in Grand Bassam inlet for a spring-neap cycle. Wet season (blue) and dry season (red)

### 4.3 Modèle Delft3D-FLOW

The less detailed Delft3D model is set up with the objective:

1. To reproduce the tidal dynamics of the lagoon system schematically
2. To investigate the inlet morphodynamics around Grand Bassam in detail

The model incorporates wave processes, sediment transport and ultimately bed updating to assess the different proposed measures to keep Grand Bassam inlet open.

#### Model setup

For the above purpose, a model grid is constructed with large detail around Grand Bassam (see Figure 4-8). The local grid resolution near the inlet is in the order of 5m to resolve the cross-section of the inlet and the surf zone dynamics adequately. In the offshore sea area and inside the lagoon, the resolution quickly coarsens in order to reduce computational times. The inlet of Canal Vridi is also incorporated in the computational grid in order to let the model resolve the distribution of the tidal volumes and river discharges over the two inlets.

The model bathymetry is again derived from the sources as presented for the FM model. The tidal boundary conditions are extracted from the FM model.

#### Hydrodynamic model validation

The Delft3D model results are validated against the FM results under the assumption that the FM model is sufficiently accurate for the study purpose. In Figure 4-9, the modeled tidal water levels at several stations are compared between the two models. It is found that, after tuning of the bottom roughness and surface area of certain lagoon branches in the Delft3D model, the qualitative performance of the Delft3D model is adequate compared to the FM model.

A further comparison of the tidal discharges is made in order to investigate whether the Delft3D model reproduces the distribution of the tidal volume and river runoff over the two inlets comparable to the FM model. Figure 4-10 presents the results for a wet season scenario with a Comoé river runoff of 550 m<sup>3</sup>/s. The discharge distribution over the two inlets is nearly similar, although Delft3d predicts slightly higher discharges at Grand Bassam and lower discharges at Canal Vridi than the FM model. However, taking into account the large model uncertainties in tidal ranges inside the system and tidal storage volumes, this difference is considered to be acceptable.

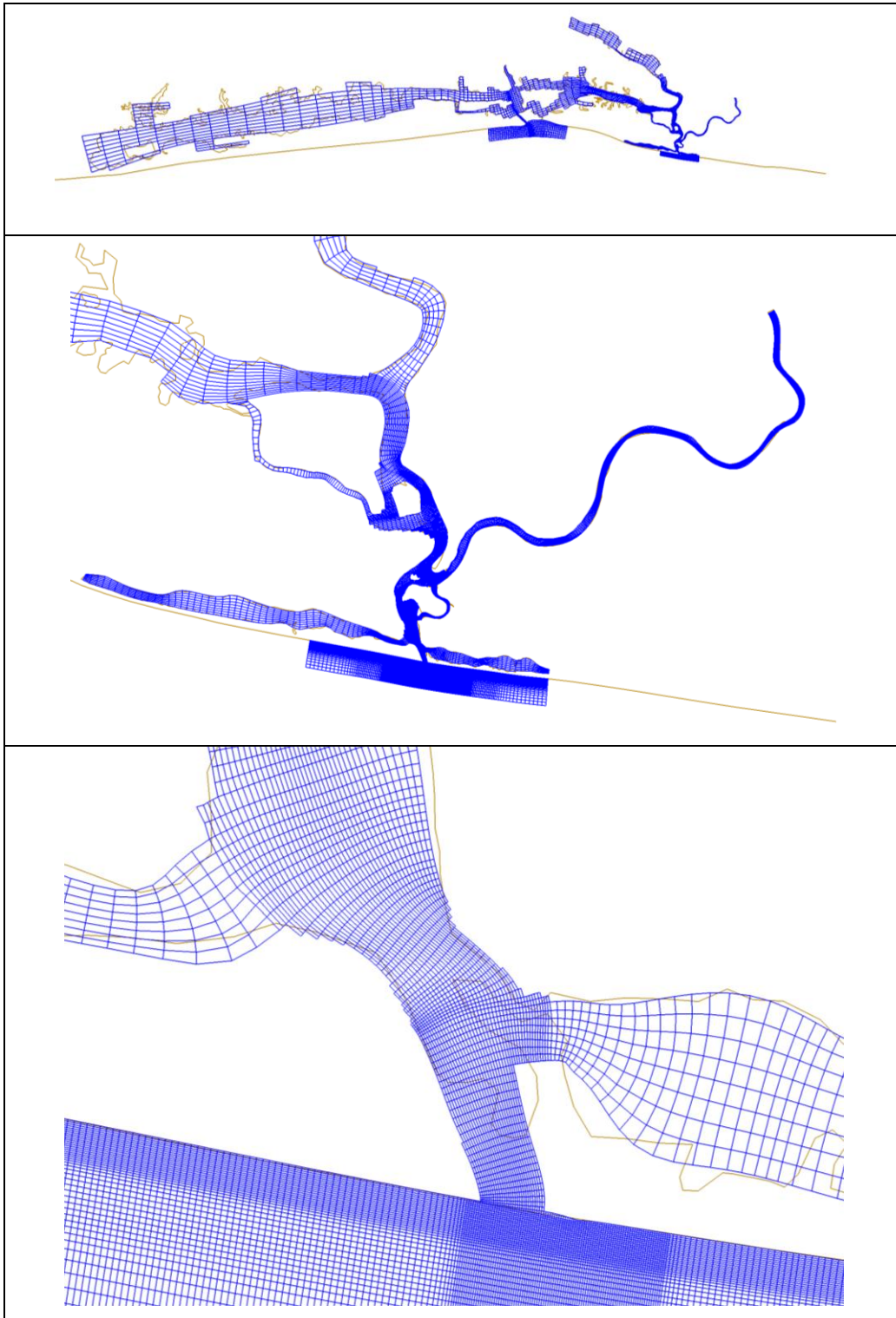


Figure 4-8 Full Delft3D model grid domain (top) and detail at the Grand Bassam inlet with increased model resolution towards the inlet (mid and bottom)

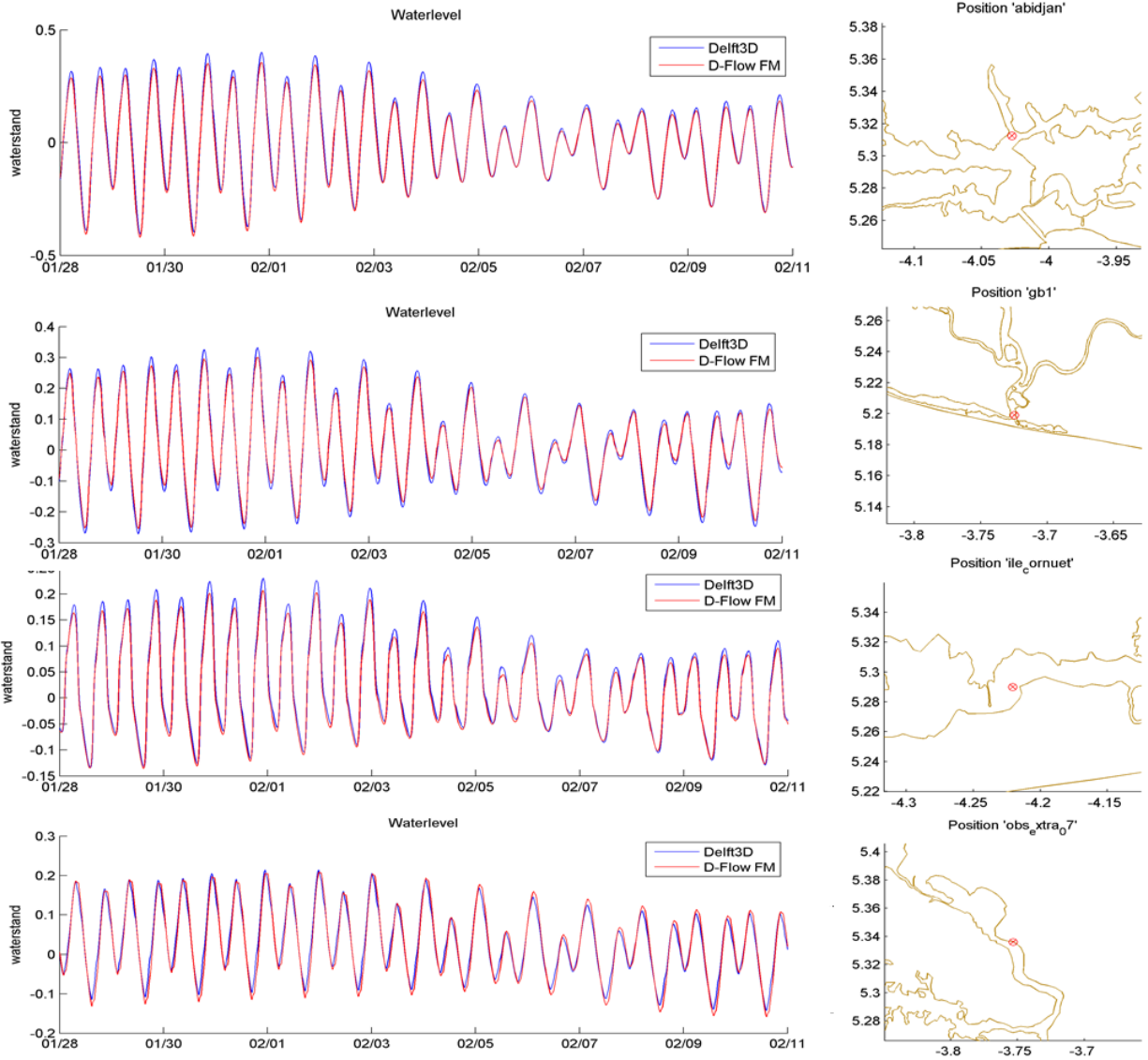


Figure 4-9 Comparison between modeled water levels of FM model (red) and Delft3D model (blue), for 4 stations in the Lagune Ebrie.

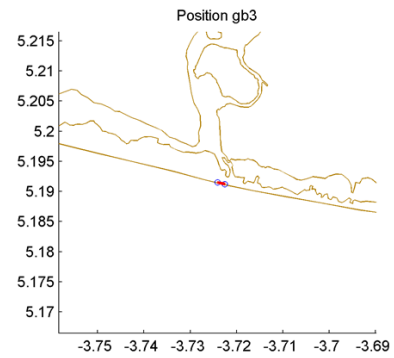
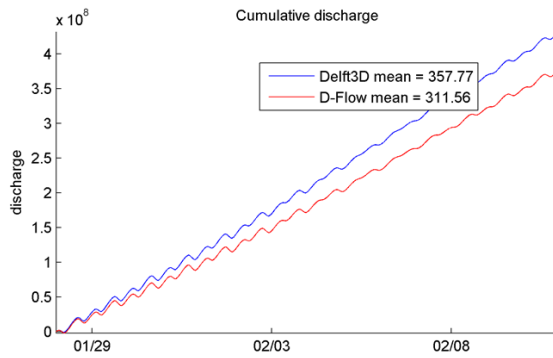
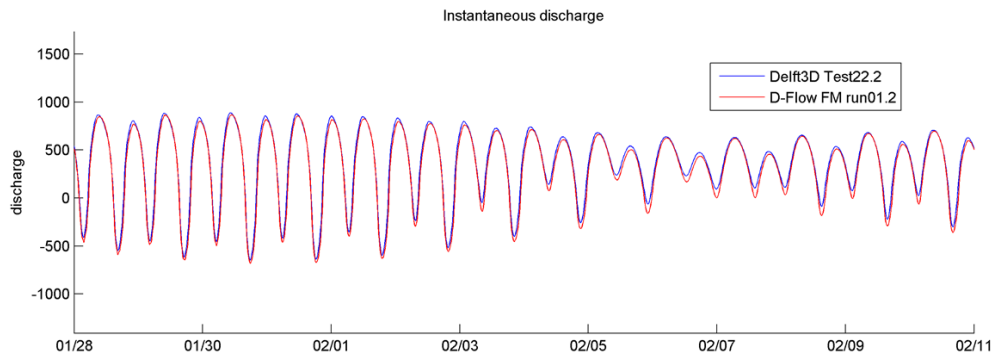
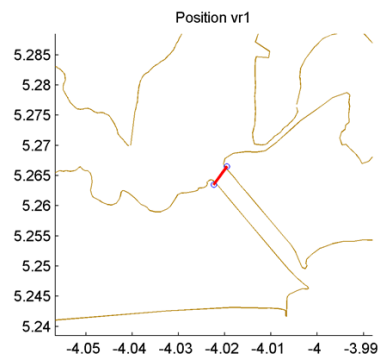
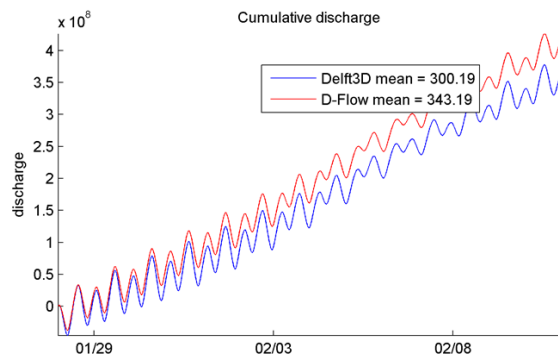
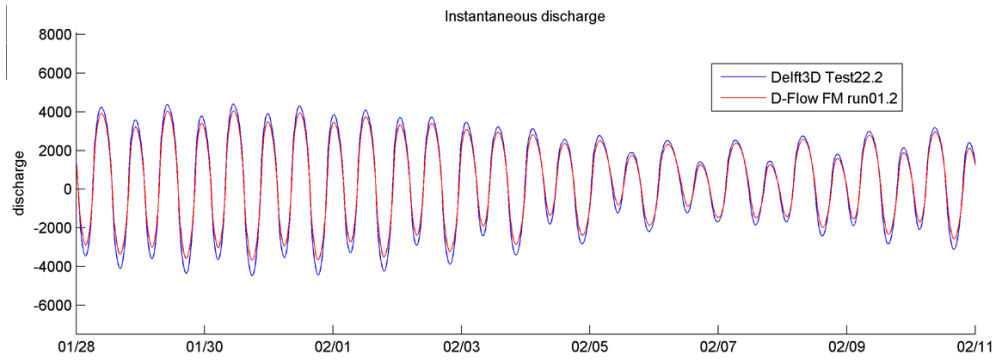


Figure 4-10 Comparison between modeled discharges of FM model (red) and Delft3D model (blue) for Canal Vridi (top) and Grand Bassam inlet (bottom).

#### 4.4 Modèle Delft3D-WAVE

A dedicated wave model is setup in order to transform the offshore wave data (NOAA data, presented in Figure xx Chapter 2) to nearshore. Figure 4-11 presents the wave model grid and bathymetry. A higher resolution nested wave grid is set up around Grand Bassam (shown in blue). The offshore wave boundary is chosen such that it coincides with the NOAA data location 4 30.00'N, 4 30.00'W, where wave timeseries are available for the period 1979-2009.

The offshore wave climate is schematized into four representative conditions, which are derived based on a classification on wave directions. Table 4-1 presents the four conditions and their yearly percentage of occurrence. Although the wave heights are comparable for the four conditions, the peak wave period increases from the southeasterly condition (1) to the southwesterly condition (4); this is related to the longer swell waves that predominantly arrive from the S-SW sector, whereas the S-SE sector also contains more locally generated wind waves. The coast normal at Grand Bassam is 190°N, which implies that conditions 1 and 2 will lead to westward directed transports for about 30% of time. Conditions 3 and 4 will generate eastward directed transports for about 70% of time.

Figure 4-12 shows an example of the computed wave heights and wave directions for condition 4. From the wave height field, wave refraction over the *Trou sans Fond* is clearly visible, leading to a localized sheltered area and increased wave heights further East.

There is no nearshore wave data available to validate the wave model results, therefore the model setup and performance is accepted as is for the present study.

Table 4-2 Schematized wave climate

Condition	Hs (m)	Tp (s)	Dir (°N)	% Occurrence
1	1.5	10	167	16
2	1.7	12	183	14
3	1.6	13	199	45
4	1.6	14	209	25

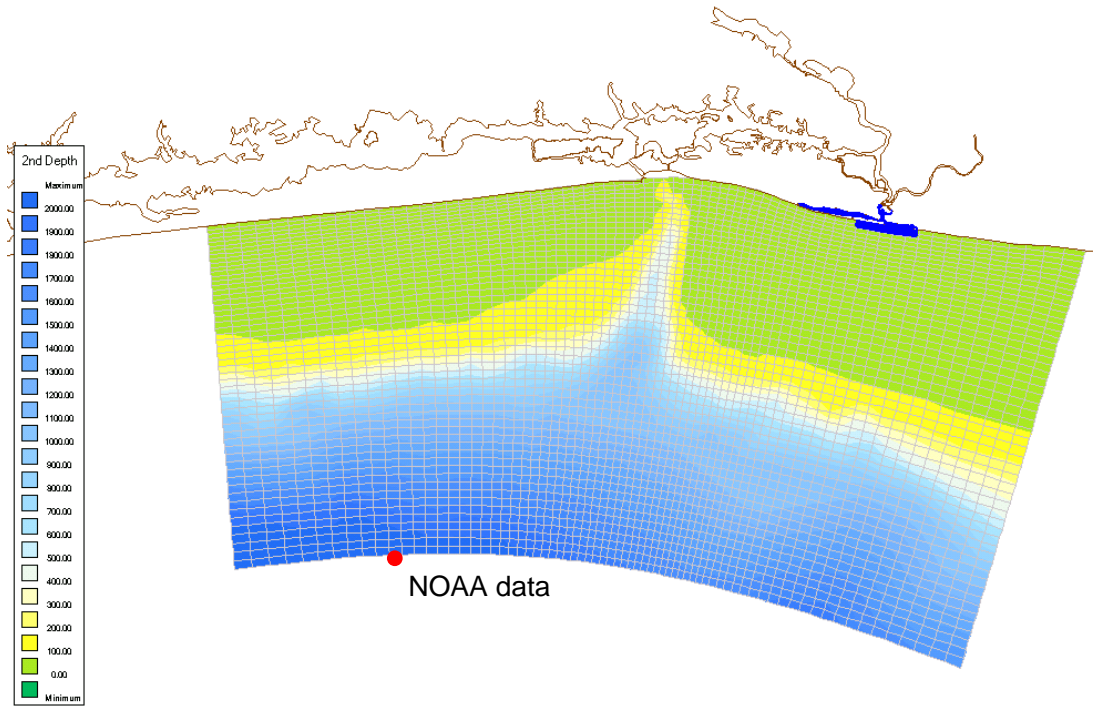


Figure 4-11 Wave model grid and bathymetry. The blue grid shows the nested high resolution wave grid around Grand Bassam.

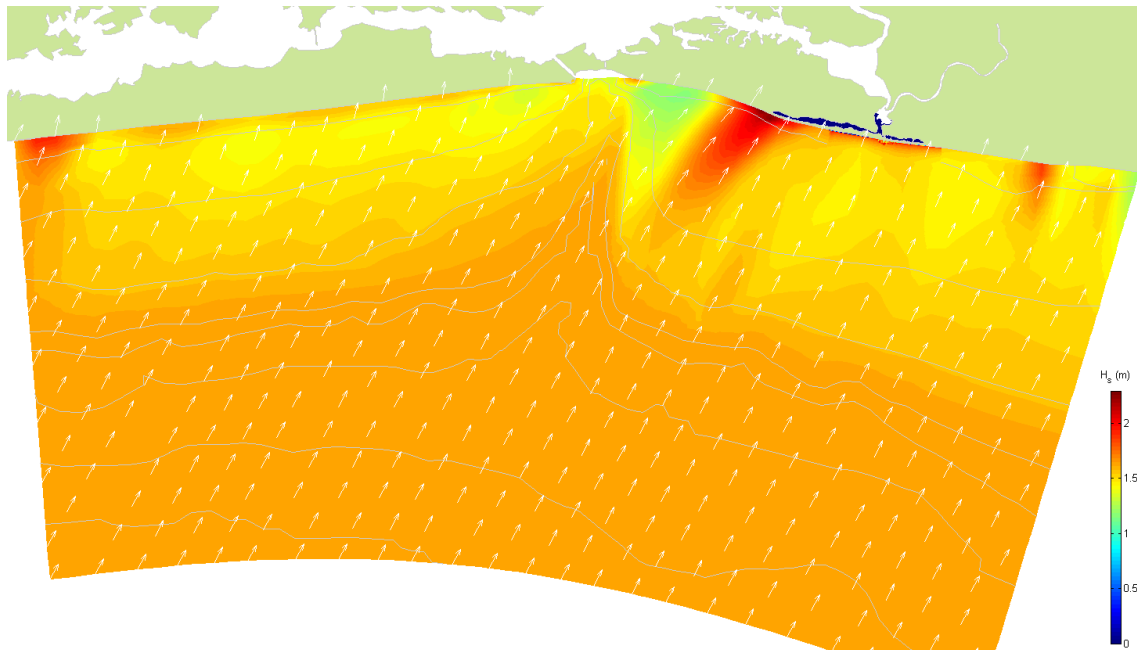


Figure 4-12 Example computed wave height field with directions (white arrows) for condition 4



## 4.5 Modèle D3D de transport

As explained in Paragraph 2.4, the Ivorian coastal zone is characterized by strong wave-driven sediment transports. This littoral transport is considered to be responsible for the closure of Grand Bassam inlet. To model the wave-driven sediment transports processes, a coupled flow-wave-sediment model is developed, which incorporates both tidal and wave-driven currents, as well as the interaction between the two processes. The objective of the model is to investigate the sediment transports in the Grand Bassam littoral region and inlet.

### Model settings

The D50 considered in the model is 500 $\mu\text{m}$ , but the large uncertainty range associated with the sediment size (see Paragraph 2.4) should be kept in mind. The transport rates are computed with the Van Rijn (1993) formulation. As wave boundary conditions, the four representative conditions as presented in the previous paragraph are considered.

### Transport results

First of all, the transports west of Canal Vridi are investigated in Figure 4-13. From the natural observed sedimentation against the harbour moles, the average longshore transport rate was estimated at a net eastward directed transport in the order of 700.000 to 1.100.000  $\text{m}^3/\text{year}$  (Sogreah, 2000).

The modelled weighted average yearly transport rates (Figure 4-13) show strongly unidirectional transports between 850.000 and 1.100.000  $\text{m}^3/\text{year}$ . These rates are derived by computing the integrated transports over the transects over a full tidal cycle for the four individual wave conditions, which are scaled to annual rates and summed taking into account the individual percentage of occurrence. The computed transports match the Sogreah estimates very well.

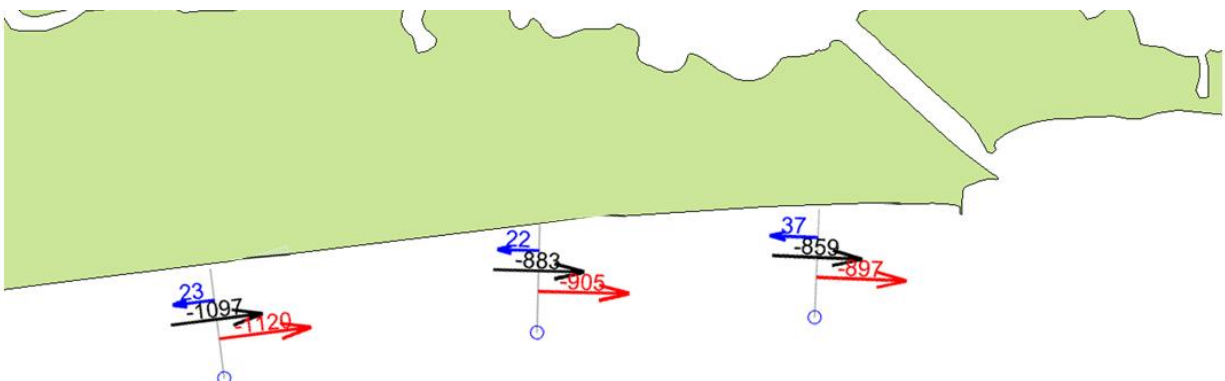


Figure 4-13 Computed longshore sediment transport rates in  $10^3 \text{ m}^3/\text{yr}$  west of Canal Vridi based on the schematized wave climate. Blue arrows indicate the gross annual westward transport, red arrows the gross annual eastward transport and black arrows the net annual transport.



Sogreah also estimated the littoral transport rates near Grand Bassam from the sedimentation against the harbour moles by taking into account the difference in coastline orientation between the Canal Vridi and Grand Bassam areas. The annual transports were estimated between 400.000 – 650.000 m<sup>3</sup>/yr in eastward direction. However, these numbers are not supported by any field observations and are in this study therefore merely considered as guideline. From the observed time to close after previous artificial openings of the inlet and known dredging figures (Paragraph 2.5), we expect that the Sogreah estimates are on the high end. We estimate deposition rates in the order of 200.000 to 400.000 m<sup>3</sup>/yr in the inlet and longshore transports of the same order of magnitude.

Figure 4-14 presents the model results near Grand Bassam inlet. The gross eastward directed transport is in the order of 200.000 to 300.000 m<sup>3</sup>/yr, whereas the gross westward directed transport is in the order of 100.000 m<sup>3</sup>/yr. The net resulting transport is therefore around 100.000 m<sup>3</sup>/yr. The deposition in Grand Bassam inlet is fed by the gross longshore transports from both directions, which totals to around 300.000 m<sup>3</sup>/yr. This figure matches the expected deposition rates well.

The predicted transport rates contain large uncertainty by lack of proper field data to calibrate or validate the model. However, from the validation of the transports West of Vridi, we conclude that the model is sufficiently adequate to reproduce the general littoral transport processes in the region.

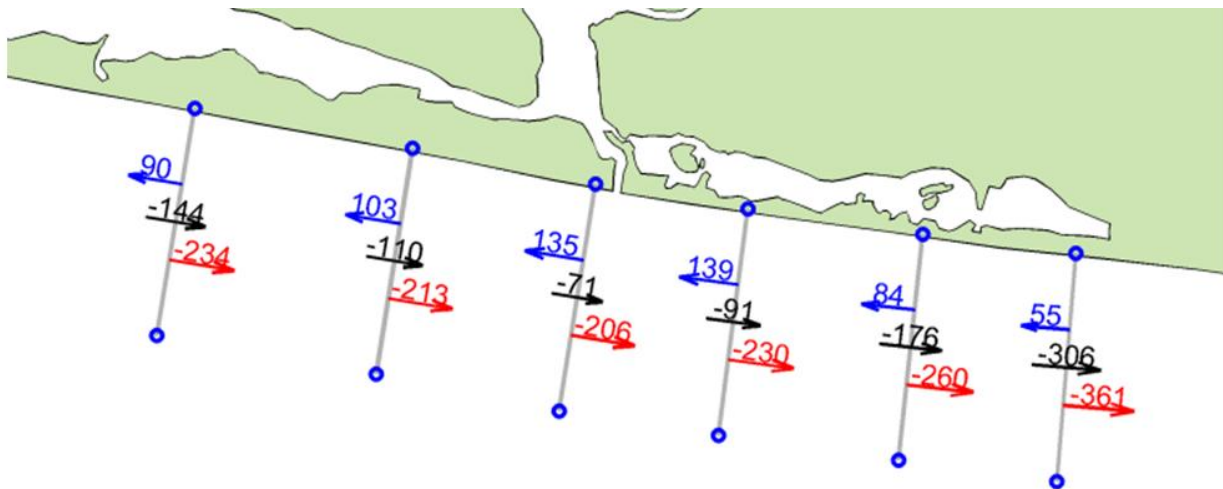


Figure 4-14 Computed longshore sediment transport rates in 10<sup>3</sup> m<sup>3</sup>/yr near Grand Bassam based on the schematized wave climate. Blue arrows indicate the gross annual westward transport, red arrows the gross annual eastward transport and black arrows the net annual transport.

## 4.6 Modèle morphologique D3D

### Approche de modélisation

To investigate the morphological development of Grand Bassam inlet, a full morphodynamic model is constructed, including tides, wave processes, sediment transports and bed updating. This model is ultimately used in Chapter 5 to assess the proposed measures to maintain the inlet open.

The aim of the model is to predict the morphological development of the inlet over a period of 1 year. As sedimentation of the inlet takes place mainly during the dry season, we reduce the simulation to the 8 months period from December to July (low Comoé discharge) and neglect the wet season, during which reopening of the inlet is expected. It is not feasible to simulate a full period of 8 months due to computational times, therefore a number of reduction techniques are used to reduce the computational effort:

1. A full spring-neap tidal cycle is reduced into a representative tide, which is commonly taken as 1.1 times the mean tidal range. In this case, a representative tidal range of 0.65 m is derived.
2. A schematized wave climate of 4 representative conditions is considered, in which the full wave climate is classified based on wave directions.
3. A significant further computational efficiency increase is obtained by simulating the separate wave conditions in parallel but simultaneously upscaling and coupling the modeled bathymetry at each flow time step. This so-called MorMerge-approach allows for relatively high MorFac upscaling factors (see bullet 4 below) as the updated bathymetry is the weighted net result of all wave conditions. Figure 4-15 presents a schematic overview of the MorMerge approach and Roelvink (2006) describes the details of this technique.
4. To further speed up the simulation, a morphological scale factor (Morfac) of 30 is used. At each time step, the computed bed level change is multiplied by this factor. By carrying out a simulation of 8 days, a full dry season ( $8 \times 30 \text{ days} = 8 \text{ months}$ ) of morphological development is obtained in this manner. The use of a Morfac is justified by the discrepancy in hydrodynamic and morphological time scales (flow responds in matter of seconds to minutes, whereas bed levels changes take place in the order of days to weeks).

### Boundary conditions

In the model, river discharges representative for the dry season are included (Comoé =  $5 \text{ m}^3/\text{s}$ , Agneby / Mé =  $25 \text{ m}^3/\text{s}$ ) and the representative tide with tidal range of 0.65m is applied. The four considered wave conditions are slightly different than those presented in Paragraph 4.4 and are representative for the dry season period only (Table 4-3).

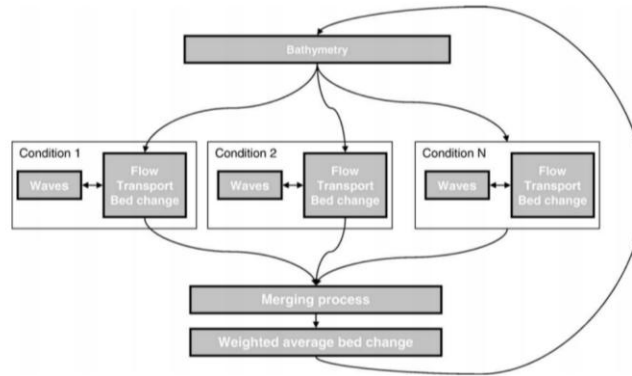


Figure 4-15 Flow diagram of the morphodynamic MorMerge-approach (Roelvink, 2006).

### Other model settings

Dans le simulation de base, un chenal initial est dragué avec largeur de 120 m, longueur de environ 500 m, profondeur de 3.5 m. Le sédiment a un diamètre median de 500 $\mu$ m et les profils de plage, par manque de données, suivent un profil théorique de Dean.

Après un nombre de simulations de calibration les résultats réalistes ont été obtenus où les profils de plage restent plus ou moins sur place sauf un léger engraissement en haut de plage. No data to further calibrate or validate the morphodynamic model.

Table 4-3 Schematized wave climate

Condition	Hs (m)	Tp (s)	Dir (°N)	% Occurence
1	1.5	10	173	25
2	1.6	13	194	25
3	1.6	13	202	25
4	1.5	14	208	25

## 5 Simulation des alternatives

With the full morphodynamic model as presented in Paragraph 4.6, the morphological development over a full dry season is evaluated for the base situation and for the 3 alternatives presented in Chapter 3:

1. Base situation
2. Continuous dredging of inlet
3. Two groynes
4. Detached groyne and sand pit

### 5.1 Alternative 0: Simulation de base

Dans les figures ci-dessous nous montrons d'abord la bathymétrie initiale pour le situation de base; dans le milieu la bathymétrie finale et en bas la distribution de l'érosion (en bleu) et de l'engraissement (en rouge), après la saison sèche qui dure 8 mois.

Our la simulation de base, qui simule le dragage d'un chenal initial sans autres mesures, un engraissement rapide est observé, menant à une fermeture complète ou presque complète dans une saison sèche. Dans les animations de l'évolution temporelle on voit clairement la propagation de bancs de sable initiés à l'embouchure vers l'intérieur, aux deux cotés du chenal. À cause de la dominance légère de vagues de l'Ouest l'engraissement dans l'embouchure est le plus fort au coté Ouest; le chenal est diminué graduellement et poussé contre le bord Est du chenal, avant d'être complètement fermé.

En général la simulation a l'air réaliste, comme ont confirmé les scientifiques Ivoiriens du Comité Interministériel. L'évolution, la forme et les dimensions des bancs de sable sont très similaires à ceux observées dans des images aériennes et satellites.

Clairement visible dans le panneau en bas est la forte érosion des côtes aux deux cotés de l'embouchure et la formation d'un delta de jusant. Cette érosion côtière a souvent été observé après des ouvertures artificielles et forme un aspect important dans l'évaluation des alternatives.

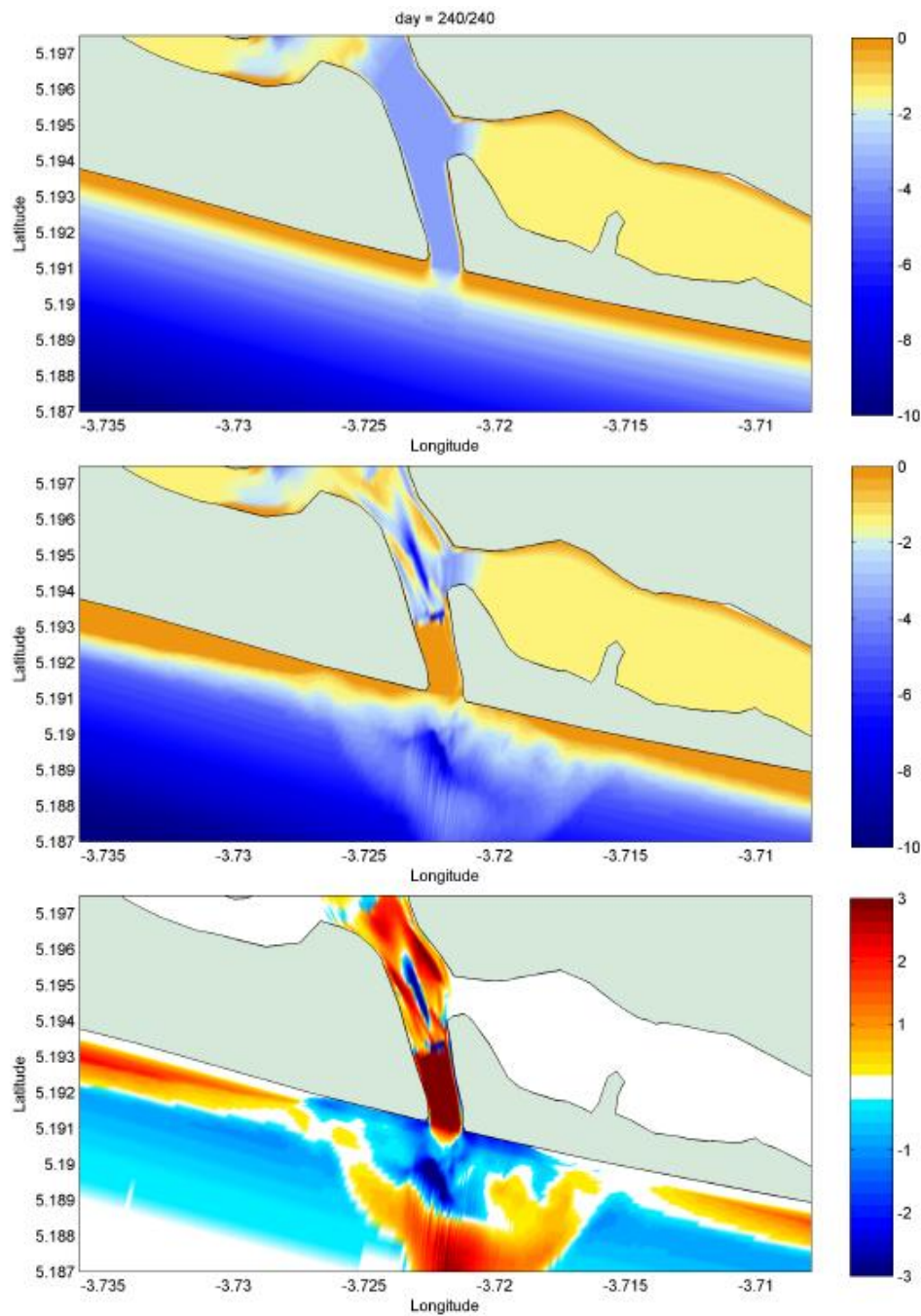


Figure 5-1 Bathymétrie initiale (haut), bathymétrie finale (milieu) et érosion/deposition (bas) après une saison sèche. Simulation de base.

## 5.2 Alternative 1: Dragage continu

Dans les simulations avec dragage continu on prescrit une profondeur minimum; si la profondeur devient moins de ça le module de dragage enlève automatiquement le volume de trop et l'ajoute au

volume cumulatif de dragage. Nous avons fait trois simulations: une avec dragage dans l'intérieur de l'embouchure (voir Figure 5-2), une avec dragage dans la partie extérieure de l'embouchure (voir Figure 5-3) et une avec dragage dans l'embouchure entière.

Dans le cas de dragage de la partie intérieure (Figure 5-2) l'effet est de juste laisser ouvert le chenal, mais avec un engraissement de l'embouchure important et une forte érosion du bord Est et des plages aux deux cotés. Cette érosion pourrait être évité par placement du sable dragué sur les plages en érosion, mais ça donnerait un gêne quasi-continu sur ces plages et mènerait probablement à une hausse de l'ensablement de l'embouchure et du volume de dragage.

Le dragage dans la partie extérieure (Figure 5-3) laisse ouverte et à profondeur toute l'embouchure mais aussi mène à une forte érosion des plages aux deux cotés.

Dans Figure 5-4 l'évolution du volume cumulatif de dragage est montré pour les trois alternatives de dragage. Clairement, dragage de la partie intérieure est associé avec des volumes les moins importants, mais encore jusqu'à 200.000 m<sup>3</sup> dans une saison sèche; dans les autres alternatives ça monte jusqu'à 500.000 m<sup>3</sup>. Il faut admettre que ce sont des volumes importants qui ne peuvent pas être déplacé par une modeste opération locale mais qui doivent être dragué par gros équipement spécialisé.

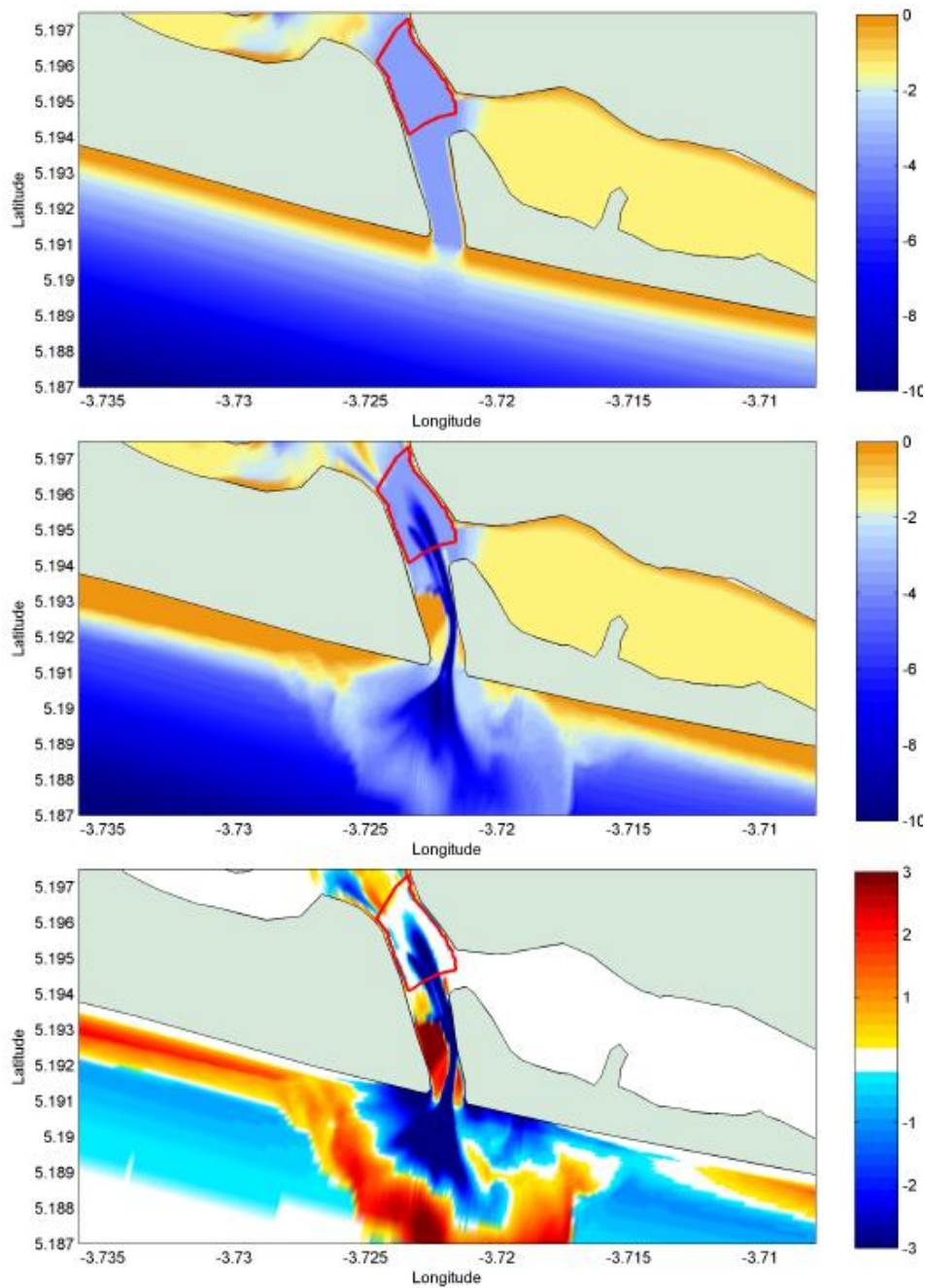


Figure 5-2 Bathymétrie initiale (haut), bathymétrie finale (milieu) et érosion/deposition (bas) après une saison sèche. Simulation de dragage continu, intérieur.



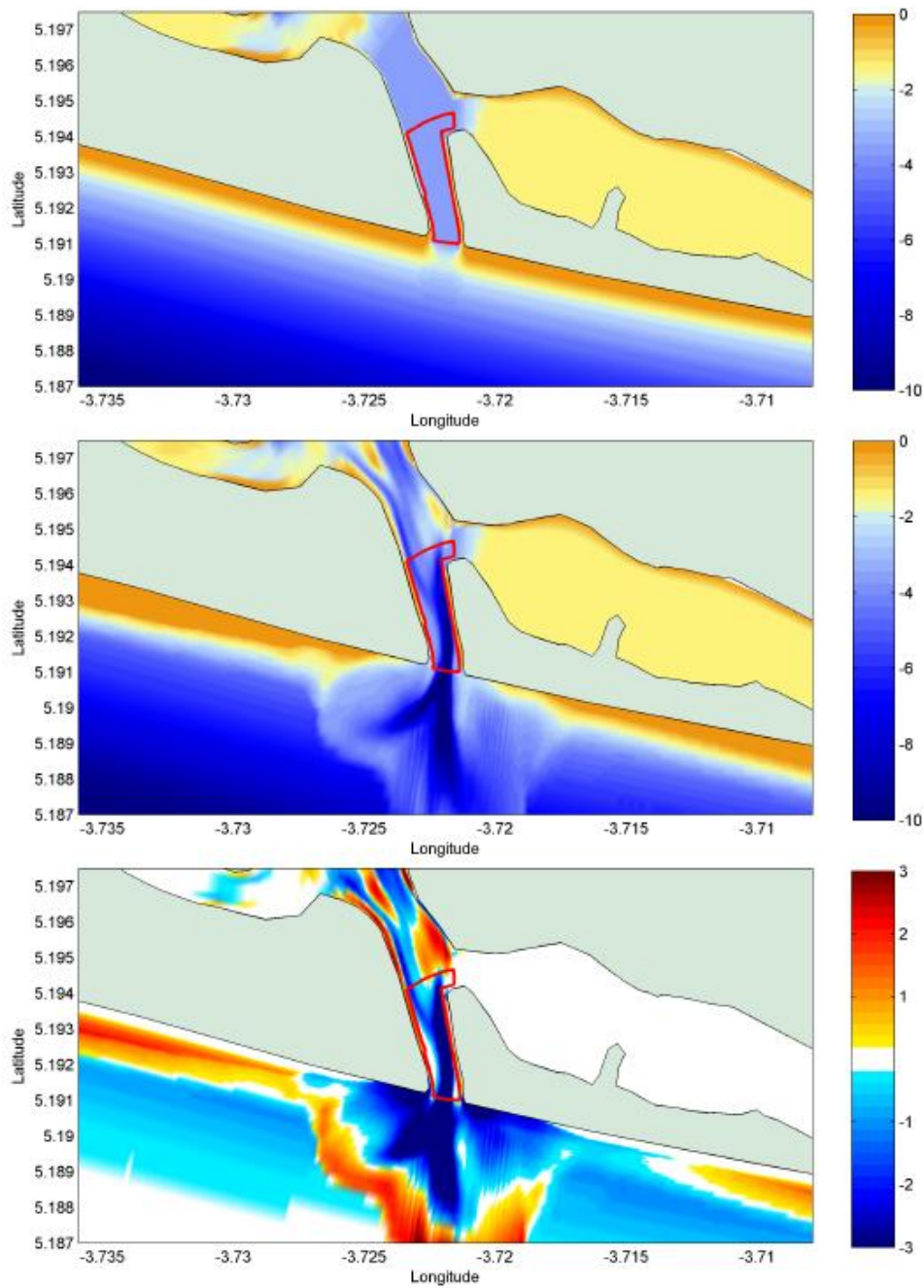


Figure 5-3 Bathymétrie initiale (haut), bathymétrie finale (milieu) et érosion/deposition (bas) après une saison sèche. Simulation de dragage continu, extérieur.



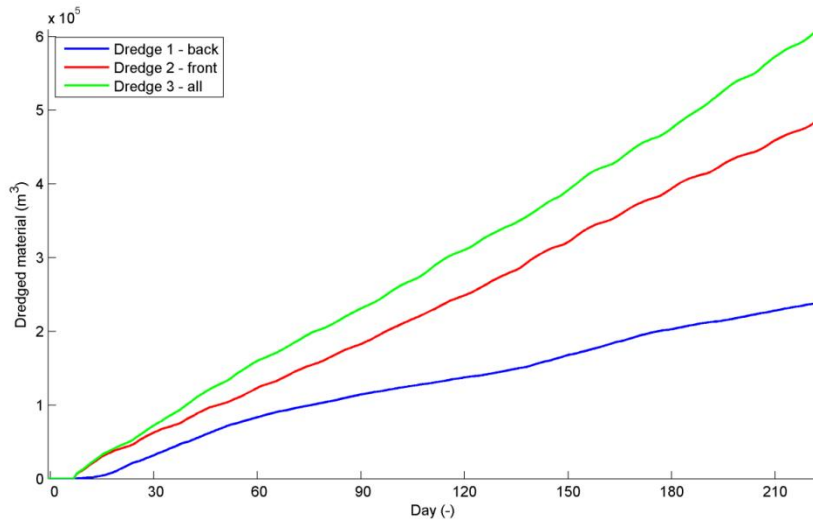


Figure 5-4 Évolution du volume de dragage cumulatif dans la saison sèche.

### 5.3 Alternative 2: Épis avec dragage d'aménagement

Dans cette option l'ensablement de l'embouchure est réduit par l'emplacement de deux épis qui bloquent le transport littoral et séparent les courants de marée et le courant littoral. L'effet de cet arrangement est montré en Figure 5-5. Il est clair qu'à la fin de la saison sèche le chenal est encore bien ouvert. À l'extérieur des épis un delta de jusant se forme à cause d'une sédimentation importante, mais reste encore bien sous la surface de l'eau. La question à répondre est en combien de temps le banc de sable se développera en manière de bloquer l'entrée. Probablement ça prendra plusieurs années, par ce que après une croissance rapide même à la fin de la première saison sèche on voit déjà des processus de 'bypass' s'installer sur le delta de jusant. À la plage Est l'érosion est modérée et pourrait bien être prévenue par un placement de sable venant du dragage du chenal initial.

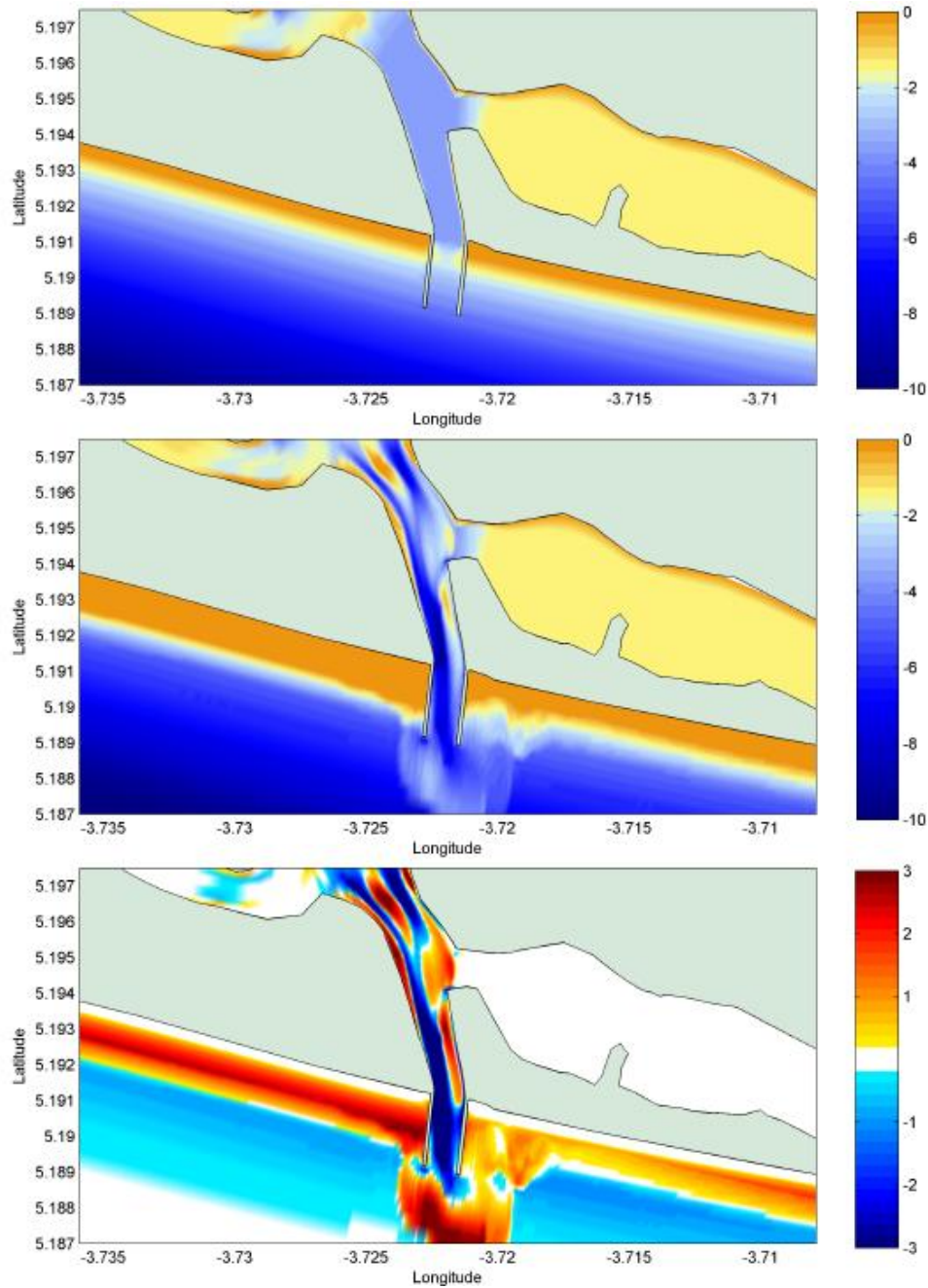


Figure 5-5 Bathymétrie initiale (haut), bathymétrie finale (milieu) et érosion/deposition (bas) après une saison sèche. Simulation de deux épis.

## 5.4 Alternative 3: Brise-lames avec piège de sable

La simulation montrée dans la Figure 5-6 ne donne pas une image optimiste sur l'efficacité de cette solution. Clairement, à cause de la nature bidirectionnelle du climat d'houles à cette location le transport venant de l'Est est encore capable d'ensabler presque complètement l'embouchure. Le piège de sable est très vite rempli et ne prévient pas l'ensablement. À la plage Est il y a une érosion importante

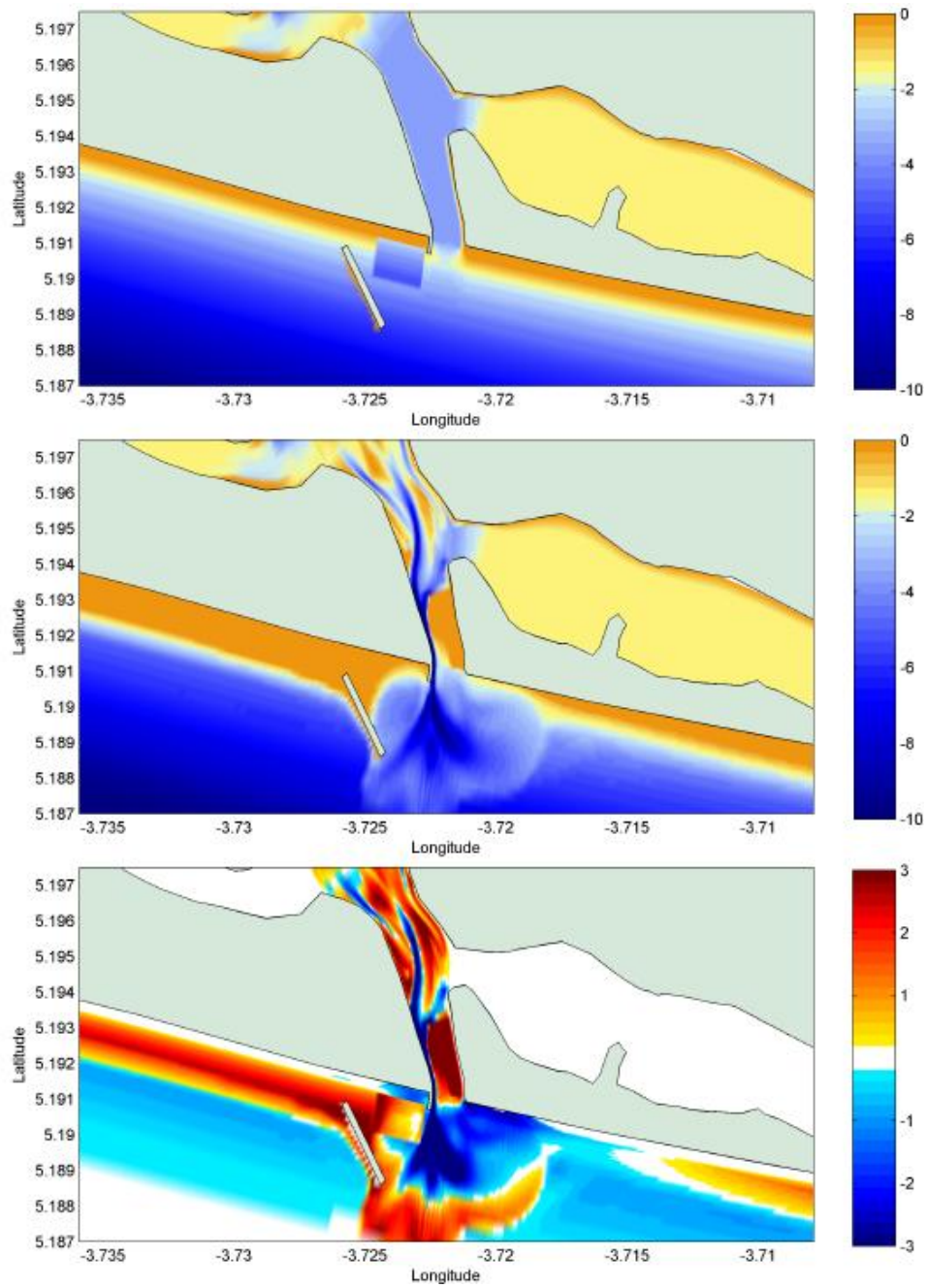


Figure 5-6 Bathymétrie initiale (haut), bathymétrie finale (milieu) et érosion/deposition (bas) après une saison sèche. Simulation avec brise-lames et piège de sable

## 6 Evaluation des alternatives

### 6.1 Critères

Pour arriver à une option préférée à base de ces simulations nous avons considéré les critères suivants:

1. L'embouchure devra rester bien ouverte après une saison sèche
2. Si dragage est nécessaire pendant la saison sèche, les volumes impliqués ne doivent pas dépasser 50.000 à 100.000 m<sup>3</sup>, afin qu'une opération locale, assez simple, puisse l'opérer.
3. L'érosion des plages devra être limitée afin qu'il ne soit pas nécessaire de supplémenter plusieurs fois par an ou de façon permanente
4. La solution choisie doit être robuste et donner la confiance qu'elle va fonctionner même après une tempête, même si une opération de dragage tombe en panne pendant une période ou si le modèle s'a trompé un peu.

Nous considérons ces critères comme primordiales: la question posée est quel option est viable en principe; d'autres considération viennent après (coût, effets secondaires)

### 6.2 Evaluation contre les critères

Nous avons évalué les options contre ces critères; évidemment l'alternative de base ne fonctionne pas, comme elle a montré dans le passé récent. Dragage seulement nécessite d'interférer pendant la saison sèche, c'est à dire plusieurs fois par an, en volumes considérables. L'alternative avec le brise-lames ne fonctionne pas sur plusieurs points et est très expérimentale. Clairement, la solution avec deux épis est la seule qui nous donne assez confiance de mener à une embouchure ouverte pérenne, même s'il sera nécessaire d'aménager la sédimentation de l'entrée et l'érosion de la plage de Mondoukou.

Critère	1	2	3	4
Alternative	Rester ouverte	Dragage pendant saison sèche	Érosion des plages	Robuste
0 - base	--		--	--
1 - dragage	+/-	--	--	-
2 - épis	++	++	+/-	+

3 - brise-lame	-	+/-	-	-
----------------	---	-----	---	---

## 6.3 Coûts globales des alternatives

RoyalHaskoningDHV

## 7 Conclusions

Une série de modèles numériques a été construit, calibré et validé de façon qualitative, afin de reproduire la propagation des marées et les courants de marée et fluviales dans tout le système lagunaire, afin de pouvoir modéliser correctement les débits et courants dans l'embouchure de Grand Bassam, en fonction du degré d'ouverture de la bouche. Cela a mené à un modèle hydrodynamique et morphodynamique assez détaillé pour évaluer de différentes options d'ouverture de l'embouchure. Ce modèle rend compte des processus des marées, débits fluviales, propagation des ondes, courant littoral, transport de sédiment et le changement de la morphologie. Le comportement de ce modèle a été validé de façon qualitative contre le comportement observé après plusieurs ouvertures artificielles dans le passé récent.

À part d'une simulation de base, trois options principales ont été évalué: dragage fréquent du chenal; deux épis avec dragage d'entretien moins fréquent, et un brise-lame avec piège de sable. À base d'un nombre de critères de viabilité, la solution avec deux épis a été choisie comme seule option à détailler dans une prochaine phase d'une étude de faisabilité.

Les résultats de l'étude décrite ici ont été présenté par Prof. Dano Roelvink de l'UNESCO-IHE au Comité Scientifique Ivoirien sur l'ouverture de Grand Bassam, qui a supporté les résultats comme assez réaliste et qui a confirmé le choix pour la solution avec deux épis.

## 8 Termes de Référence d'une étude de faisabilité

### 8.1 Modélisation détaillée et probabiliste de l'option choisie

#### 8.1.1 Validation de la performance du modèle

#### 8.1.2 Prévision de développement moyenne sur plusieurs années

#### *Dimensionnement de l'ouvrage*



*Fréquence et ampleur de dragage*

*Interventions pour l'atténuation de l'érosion*

**8.1.3 Variations saisonnières et interannuelles**

**8.1.4 Effet de conditions extrêmes**

**8.1.5 Étude de stabilité de l'ouvrage**

**8.1.6 Évaluation des effets hydrauliques et morphologiques du projet**

## **8.2 Étude de l'impact environnemental et social**

**8.2.1 Collection de données sur la situation présente**

**8.2.2 Estimation des paramètres possiblement impactés**

**8.2.3 Modélisation des paramètres et validation pour la situation existante**

**8.2.4 Simulation des impacts des mesures proposées**

*Développement autonome*

*Alternative de préférence*

*Alternative le plus adapté à l'environnement*

*Alternative le plus économique*

**8.2.5 Analyse des impacts socio-economiques**

*Plages*

*Inondations*

*Pêche*

*Port de plaisance*

*Développement touristique*

*Enjeux*

*Faune et flore*

*Patrimoine culturelle*

*Valeur marchande des terrains et des bâtiments*

**8.2.6 Analyse et avis sur les impacts**

**8.3 Estimation de coûts initiaux et récurrents**

**8.4 Préparation de plans détaillés**

**8.4.1 Proposition d'un plan d'aménagement de la zone d'étude.**

**8.4.2 Préparation de plans de construction des structures**

**8.4.3 Préparation d'un plan de gestion des sédiments côtiers**

**8.5 Formation de capacité en exécution de suivis**

**8.5.1 Suivis bathymétriques en fonction du comportement du chenal**

**8.5.2 Courantométrie**

**8.5.3 Salinité, concentration, température**

**8.5.4 Qualité d'eau**

**8.5.5 Écologie**

**8.5.6 Dynamique de la population**

**8.6 Préparation de documents d'appel d'offre**

**9 Littérature**

Roelvink, J. A. (2006). "Coastal morphodynamic evolution techniques." Coastal Engineering 53(2–3): 277-287.